HIGH THROUGHPUT DETERMINATION OF ETHANOL IN ALCOHOLIC BEVERAGES BY USING IMAGE PROCESSING WITH MODIFIED 96-WELL MICROPLATE

MR.VIJAK KHUPVIWAT
MS.WALAILUK ERB-ARB
MS.NUTCHUDA SAECHUA

A SPECIAL PROJECT SUBMITTED IN PARTIAL FULFILLMENT
OF THE REQUIRMENT FOR THE DEGREE OF BACHELOR OF SCIENCE
IN PETROCHEMICAL TECHNOLOGY
FACULTY OF SCIENCE
KING MONGKUT'S INSTITUTE OF TECHNOLOGY LADKRABANG
ACADEMIC YEAR 2011

Title High Throughput Determination of Ethanol in Alcoholic Beverages By Using Image Processing with Modified 96-well Microplate

Students Mr.Vijak Khupviwat

Ms.Walailuk Erb-Arb

Ms.Natchuda Saechua

Degree Bachelor of Science

Major Program Petrochemical Techonology

Academic Year 2011

Advisor Dr.Nathawut Choengchan

ABSTRACT

The purpose of this research is to develop a new analytical method for determination of ethanol in alcoholic beverages. The main advantages of this method are high throughput and cost saving by using a 96-well microplate and digital camera as detector. The colorimetric reaction between dichromate and ethanol was observed. A modified 96-well microplate was used to carry samples (ethanol) and reagents (dichromate) in a pair of wells, hence 18 samples can be measured at the same time. After samples and reagents were pipette into wells, the microplate was put into oven for 7 minutes at 70 °C. Seven minutes later microplate was taken out then takes a photo after 30 sceond using digital camera. The image of sample was processed by software Image_J to measure the intensity of red color. The intensity is then used to calculate reflectance. Calibration curve was made by the linear relation between reflectance and percentage of ethanol. Caliration equation was found to be $y = (0.0346 \pm 0.0057)\,x - (0.1144 \pm 0.0844)$. Linear working range was 5-40 % (v/v) ethanol. Limit of detection was 1.99 % (v/v) ethanol. The precision study shows poor RSD value due to poor temperature distribution in the oven. However, for further development more factors should be investigated

Key words: Image processing / alcoholic beverages / modifired 96-well microplate / ethanol analysis

ACKNOWLEDGEMENT

Firstly, we would like to thank Dr.Nathawut Choengchan for warmly advising, teaching, and encouraging our group to successfully finish this special project. We would like to give credit for him who gives many valuable suggestions, a source of contribution and encouragement.

Thanks to Dr.Saowapak Teerasong and Dr.Tipachai Vatanavicharn for valuable comment and suggestion in completion of the special project.

Thanks are also gone to Asst.Prof.Dr.Naratip Vittayakorn for his kindness contribution on using heating oven.

We would like to thanks to Faculty of Science, King Mongkut's Institute of Technology Ladkrabang, for providing us many usefull instrument in this project. Further thanks to staffs and personnels is this Faculty for help us.

Other thanks are belonges to graduated students in researcher group of Dr.Nathawut Choengchan for many warmly helps, advices, and ideas for this project.

Last but not least, we would like to express them the deepest appreciation to our dearest father, mother, relatives, and friends for loves, cares, and encouragement that they gave us, which is the most importance in life

Finally, thanks our project team for everything that we have done and share together.

Mr.Vijak Khupviwat

Ms.Walailuk Erb-Arb

Ms.Nutchuda Saechua

CONTENTS

CONTENTS (Continued)

Page

CONTENTS (Continued)

Page

LIST OF TABLES

LIST OF TABLES

Table **Page**

LIST OF FIGURES

LIST OF FIGURES (Continued)

Figure **Page**

LIST OF FIGURES (Continued)

LIST OF FIGURES (Continued)

LIST OF ABBREVIATIONS

°C	Celsius degree
°F	Fahrenheit degree
i.d.	Inner diameter
cm	Centimeter
mm	Millimeter
nm	Nanometer
mg	Milligram
g	Gram
μL	Microliter
L	Liter
mL	Milliliter
μL	Microliter
dm^3	Cubic decimeter
s	Second
min	Minute
h	Hour
$mol.L^{-1}$	Molar
GC	Gas chromatography
GD	Gas diffusion
MGD	Membraneless gas diffusion
RSD	Relative standard deviation
SD	Standard deviation
r^2	Correlation coefficient
et al.	Et Alli (Latin), and others
eV	Exposure value
M	Molar
EtOH	Ethanol
ISO	The International Organisation for Standardization
LOD	Limited of detection

CHAPTER I

INTRODUCTION

1.1 Alcoholic beverage

An alcoholic beverage is a drinkable liquid that contain ethyl alcohol or ethanol which is a volatile organic compound. Alcoholic beverage can be divided into 2 groups. The first group is distilled fermented beverages such as whisky, brandy and liquors. Another group is un-distilled fermented beverages such as beer and wine [1].

1.2 Types of alcoholic beverages

Alcoholic beverage was classified into 5 parts based on their manufacturing process and alcoholic content as summarized in Table 1.1.

Table1.1. Summary and classification of alcoholic beverages [2].

Class of alcoholic beverage	Type of alcoholic beverage	Description	Alcohol content (% v/v)
Distilled fermented beverage	Whisky	Made by distilling the fermented juice of grains such as corn, rye or barley.	40-55
	Brandy	Made by distilling the fermented juice of fruits and collected in oak tank.	40-50
	Liquors	Made by distilled the grain mixing with sugar or sugarcane and fermented mash.	40
Un-distilled fermented beverage	Wine	Made from a variety of fruits, e.g. grapes, peaches or plums. Fruits are crushed and fermented in a large container for months or years result in production of alcohol.	5-23
	Beer	Made from a grain of cereals, corn, wheat or barley and mix with yeast.	4-8

1.3 Manufacturing of alcoholic beverage

According to types of alcoholic beverages, the distilled fermented beverages contain higher alcohol content than that of the un-distilled fermented beverages as shown in Table1. Both groups acquired anaerobic reaction for fermentation as shown in equation (1) [3-5].

$$C_6H_{12}O_6 \xrightarrow{\text{Yeast}} 2C_2H_5OH + 2CO_2$$

Sources of the distilled fermented beverages are fruits or starch of plant while sources of the un-distilled fermented beverages are juice of cereal grain or sugar cane (Table1.1). For the distilled fermented beverages, natural sugar is easily converted to ethanol and after that followed by distillation method. The distillation process is based on difference between boiling point of water (212°F or 100°C) and ethanol (173°F or 78.5°C). While fermented liquid boils, the ethanol vapor is trapped and re-condensed to create liquid of concentrate ethanol. The process of distillation method and photograph of instrumental set up are shown in Figure 1.1 and Figure1.2, respectively.

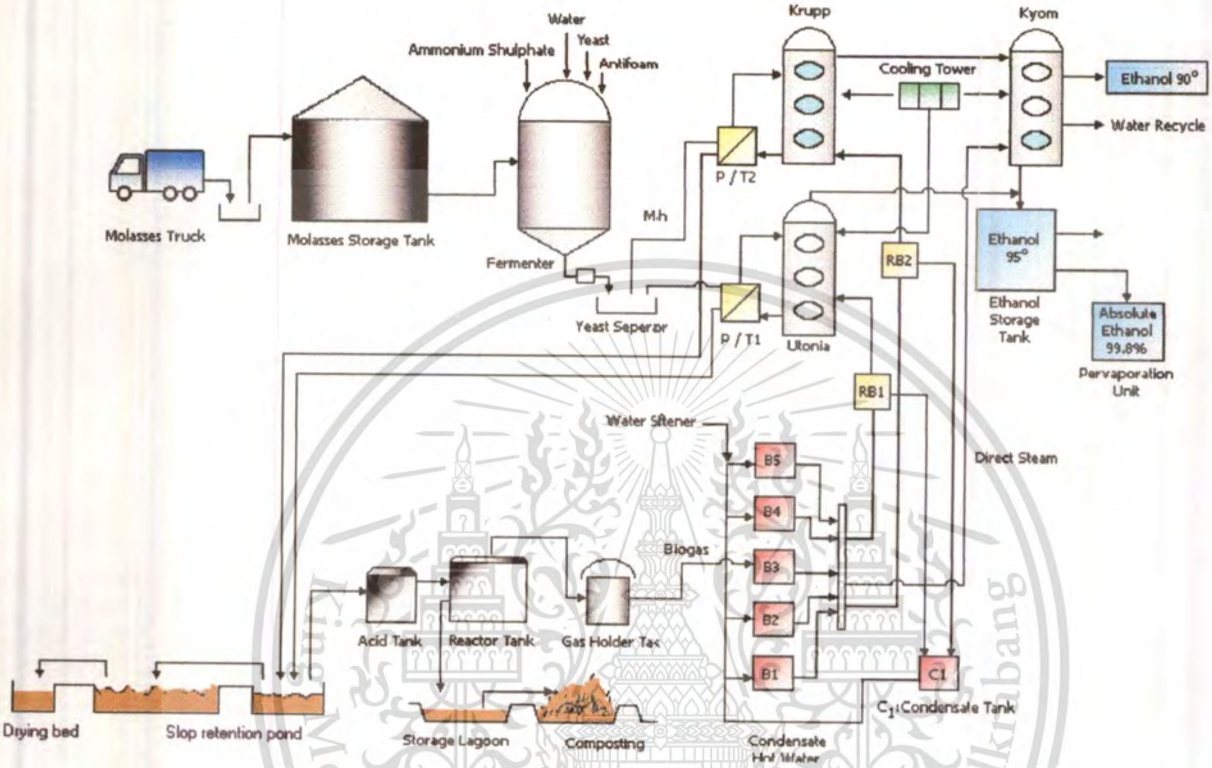

Figure1.1 Schematic diagram of the production process of ethanol [6]

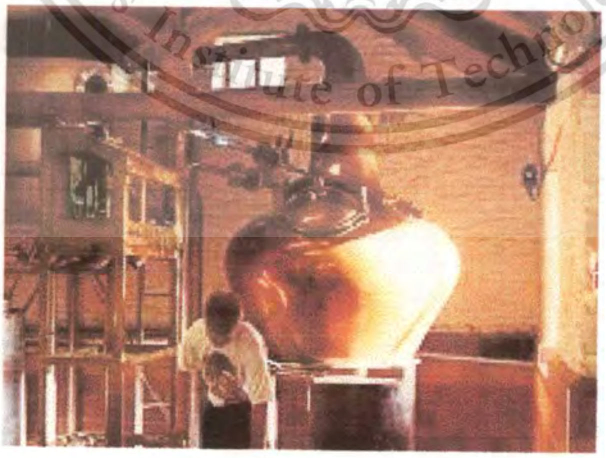

Figure1.2 A photograph of instrumental setup in brandy industry [7].

1.4 Regulation of alcoholic beverage in Thailand

Ethanol content plays an important role for quality and classification of alcoholic beverages. According to legislative requirement of Thailand Industrial Standard Institute (TISI), Ministry of Industry, the controlled level of ethanol content in alcoholic beverages are concluded in Table 1.2.

Table1.2 Controlled levels of ethanol concentration of some parameters in alcoholic beverages [8-9].

Parameter	Controlled level of concentration	Type of alcoholic beverage
Ethanol	5 to 22 % (v/v) 0.5 to 80 % (v/v)	Un-distilled fermented beverage Distilled fermented beverages
Fuel oil	2,500 mg dm^{-3} 5,500 mg dm^{-3}	Un-distilled fermented beverage Distilled fermented beverages
Methanol	420 mg dm^{-3}	Both of un-distilled fermented beverage and distilled fermented beverages
Acetaldehyde	160 mg dm^{-3}	Both of un-distilled fermented beverage and distilled fermented beverages
Ethyl acetate	1,200 mg dm^{-3}	Both of un-distilled fermented beverage and distilled fermented beverages

1.5 Charge Coupled Device (CCD)

A charge-coupled device (CCD) is a device for the movement of electrical charge, usually from within the device to an area where the charge can be manipulated, for example conversion into a digital value. This is achieved by "shifting" the signals between stages within the device one at a time. CCDs move charge between capacitive bins in the device, with the shift allowing for the transfer of charge between bins.

The CCD is a major technology for digital imaging. In a CCD image sensor, reverse-biased p–n junctions (essentially photodiodes) are used to absorb photons and produce charges representing sensed pixels; the CCD is used to read out these charges. Although CCDs are not the only technology to allow for light detection, CCD image sensors are widely used in professional, medical, and scientific applications where high-quality image data is required.

In a CCD for capturing images, there is a photoactive region (an epitaxial layer of silicon), and a transmission region made out of a shift register (the CCD, properly speaking).

An image is projected through a lens onto the capacitor array (the photoactive region), causing each capacitor to accumulate an electric charge proportional to the light intensity at that location. A one-dimensional array, used in line-scan cameras, captures a single slice of the image, while a two-dimensional array, used in video and still cameras, captures a two-dimensional picture corresponding to the scene projected onto the focal plane of the sensor. Once the array has been exposed to the image, a control circuit causes each capacitor to transfer its contents to its neighbor (operating as a shift register). The last capacitor in the array dumps its charge into a charge amplifier, which converts the charge into a voltage. By repeating this process, the controlling circuit converts the entire contents of the array in the semiconductor to a sequence of voltages. In a digital device, these voltages are then sampled, digitized, and usually stored in memory; in an analog device (such as an analog video camera), they are processed into a continuous analog signal (e.g. by feeding the output of the charge amplifier into a low-pass filter) which is then processed and fed out to other circuits for transmission, recording, or other processing [10].

Figure1.3 A specially developed CCD used for ultraviolet imaging in a wire bonded package.

1.6 OBJECTIVE

1.6.1 To design and develop image processing as selective analytical method for determination of ethanol.

1.6.2 To investigate the validity of methods for quality control of alcoholic beverages by monitoring ethanol concentration.

CHAPTER II

LITERATURE REVIEWS

Various analytical methods were developed for analyzing ethanol in alcoholic beverage. In this chapter, the methods for determination of these were briefly reviewed in the following parts.

2.1 Chromatographic method

Normally, Gas chromatography (GC) has been the most widely used method for ethanol analysis. An official method of the association of official analytical

chemists (AOAC) was employed with flame ionization detector and used a glass column packed with 0.2% Carbowax 1500 on 80-100 mesh Carbopack C was employed [12].

Capillary gas chromatography was used for direct injection of sample after added a proper amount of internal standard. The method provided a simple and rapid technique to determine ethanol in alcoholic beverage. This method was proposed by M. Wang, *et al.* in 2003 [13]. The method could change the concentration in gravimetric percent (%, w/v) to volumetric percent (%, *v/v*) by the equation (%, w/v) = 0.814 (%, *v/v*) with linear coefficient $r^2 = 0.999$ and analysis time less than 8 min. In the following year, a simultaneous quantification of the methanol and ethanol in alcoholic beverage was presented by the same group [14]. This work was used a mega-pore capillary column (CP-wax 58 CB) with FID detector. The sample was spiked with double internal standards as 100 μg 2-pentanol and 50 mg acetonitrile. One shot analysis was determination of ethanol and methanol. The data was record less than 12 min.

In 2009, Haillong Li *et al.* [15] also presented a rapid and simple method by full evaporation headspace gas chromatography for determination of ethanol in fermentation liquor. The equilibration time was almost completely within 3 min at a temperature 105 °C.

For liquid chromatography technique (LC), high-performance liquid chromatography-flame ionization detection with a mobile phase which is a pure water and use of a C_{30} silica gel as a stationary phase was presented by T. Yarita *et al.* [16]. The advantages of method are, quantify the concentration of ethanol in six kind of alcoholic beverages and no significant change in the retention time of alcohol in period time for 96 h.

A high-performance liquid chromatography couple with diamond attenuated total reflection (ATR) -Fourier transform infrared (FTIR) spectroscopy detection was reported [17]. The volume of 50 µl of red wine sample was analyzed. The liquid chromatography technique was separated of organic acids, sugar and alcohol content. And the unique finger print of sample is used for the confirmation of analyte by FTIR. The separation ion-exchange column was used with a 0.005 mol L^{-1} sulfuric acid as a mobile phase [18]. An ATR cell was coated by a thin film of polymer to avoid an acidic degradation from mobile phase.

2.2 Electrochemical Method

Many techniques of biosensor for ethanol determination using electrochemical method have been reported. In 2006, an electronic tongue was used with potentiometric response of pophyrin-base membrane which a film was detailed by co-ordination interactions happening between ethanol and the free ligand site metal for alcohol by L. Lvovao *et al.* [19]. The application of electronic tongue system was not only for classification of alcoholic degree of beverage but also for testing the chemical composition of final product.

In the same year, the amperometric biosensor was also attractive for analysis of ethanol [20]. The response of amperometric was based on the electro catalytic properties of meldola's blue (MB) which modified carbon electrode was called muti-wall carbon nanotube (MWCT) to oxidize NADH that generated by enzymatic reaction of ethanol with NAD^+. Linearity range was found in concentration range of 0.05 – 10 mmol L^{-1}.

In 2008, the muti-walled carbon nanotubes was used to develop an alcohol oxidase (AlcOx) biosensor and applied in a glucose-oxidase-based biosensor (GOx).

Ethanol biosensor was monitored amperometrically at -0.30 V vs. SCE at pH 7.5 and the sensitivity was 20 times higher than another biosensor without muti-walled carbon nanotube (MWCNT) [21].

2.3 Spectrometric Method

Several of publications for determine ethanol based on spectrometry methods have been presented.

Determination of ethanol and methanol using an enzymic method was presented by M. Ulyana *et.al.* The reaction of alcohol oxidation catalysed by alcohol oxidase conjugated with the indicator reaction of p-phenylenediamine oxidation with hydrogen peroxide was selected. The absorbance was measured at 540 nm 20 min after the addition of p-phenylenediamine oxidation and alcohol oxidase solutions. The determination of ethanol and methanol with limit of detection was 9 µmol L^{-1} and 0.9 µmolL^{-1}, respectively [22].

Fourier transform infrared (FTIR) spectrometric detection was also used for measurement of ethanol. M. Gallignani *et.al.* [23] studied the quantitative ethanol include on- line liquid –liquid extraction with chloroform, through a sandwich type of two channel cell that was rely on PTFE membrane. The organic phase was measured by FTIR. The sample no need to preparation except for degas of beer and gassy wine.

This work was proposed by A.D. Magri *et al.* [24]. Chromium (VI) was react with ethanol in 100 µl of alcoholic beverage sample that form chromium (III) and acidic. Decrease of chromium (VI) content in perchloric acid solution was determined by absorbance at 267 nm. The reaction time was completed within 15 min.

Another application of oxidation has been applied with bioethanol process by H. B. Seo *et al.* [25] Samples were extracted by tri-*n*-butyl phosphate solution, which is solvent extraction before reacted with dichromate. 96-deep well plate was contained with aqueous phase and dichromate reagent that measured a product with microplate reader at 595 nm.

2.4 Techniques for high throughput analysis

Normally, flow-based technique has advantages such as automization analysis and minimization in the required volume of sample a. Many researchers have published various applications of this technique for determination of ethanol.

P. Tipparat *et al.* [26] proposed the FI-NIR system for determination of ethanol in liquor. A liquor sample was equilibrated off-line with dried chloroform to extract ethanol into organic phase. The extract was then injected into the FI system passing through a homemade flow cell (1-cm path length) for continuous monitoring of absorbance at 2,305 or 2,636 nm. The method provided a linear calibration in the concentration range of 20-50 % *(v/v)* ethanol and the sample throughput is 240 sample h^{-1}.

The determination of ethanol in distilled liquors was proposed in sequential injection analysis (SIA) by P. J. Fletcher *et al* [27]. The reaction of acidic potassium dichromate mixing with ethanol was used. The determination of sample was use 200 µl and measured at wavelength 600 nm. The linearity range of this method is up to 6% *(v/v)* $r^2 = 0.9995$ with a detection limit 0.09% *(v/v)* and the sample throughput is 19 sample h^{-1}.S

S. Sivannildo *et al.* [28] proposed the procedure of a falling drop of red wine for determine ethanol by infrared LED ($\lambda = 935$ nm) and a phototransistor (Til78) detection. The wine drop was generated between detection devices that could be absorption and/or scattering signal from infrared radiation beam, and then make a decrease of intensity of radiation beam start from the LED. A linearity range 1 to 30 % *(v/v)* ethanol $r^2 = 0.999$ and detection limit is 0.3% *(v/v)* ethanol. The sampling rate is 50 determinations per hour.

Spectrometric-enzymatic method has been presented for quantitation of ethanol. A sequential injection system was developed to enzymatic reaction catalyzed by alcohol dehydrogenase in the presence of NAD that was presented by R. N. M. J. Pascoa *et al.*[29]. This work used 50 µL of wine sample, and the reaction of alcohol dehydrogenase was measured absorbance at 340 nm and the determination rate was 25 samples per hour.

The sequential injection lab-on-valve (SI-LOV) format for the miniaturization of enzymatic assays was presented by S. S. M. P. Vidigal *et al.*[30]. The different measurement modes of peak height and initial rate were used. Both of peak height and initial rate-based were gave the linearity range up to 0.040 % *(v/v)* and good repeatability. The determination rate achieved was 37 and 27 determinations h^{-1} for the initial rate and for the peak height measurement, respectively.

A microfluidic device has been presented for quantitative ethanol in wine and beverage. L. Lei *et al.* [31] described use of direct reaction of ethanol that diluted and potassium dichromate in sulfuric acid. Green product of reaction was detected by absorbance at 600 nm. Working range for ethanol between 0 to 6 % (v/v) could be achieved.

A trend of flow-based and technique with membrane-based gas diffusion were widely employed in flow technique for ethanol determination, a volatile analyte be able to separated from interference through gas diffusion process across a hydrophobic membrane, which are gas diffusion and pervaperation. For membraneless gas diffusion, a gaseous analyte can be vopour via a small head space, which created between sample container and acceptor container in close system. All of those processes in the previous were a selective because only a volatile of ethanol is converted to gaseous from a room temperature.

In 2006, N. Choengchan *et al* [11] developed a new design gas diffusion unit, called 'membraneless gas diffusion (MGD) unit' (Figure 2.1). The unit does not rely on use of hydrophobic membrane. A unit has two grooves of parallel channels inside the closed module. These grooves were used for flowing donor and acceptor stream. The two channels have a barrier between them, which is slightly lower height than the depth of the channel. So a volatile compound can vaporize across this barrier from donor side to acceptor side. The selective of volatile analyte was separated without use of any porous membrane. This MGD unit was applied for determination of ethanol in alcoholic beverages. The detection based on photometry of dichromate reduction by vapor of ethanol. Detection limit was lower than the Gas diffusion (GD: 0.68% *(v/v)*; MGD: 0.27% *(v/v)*)

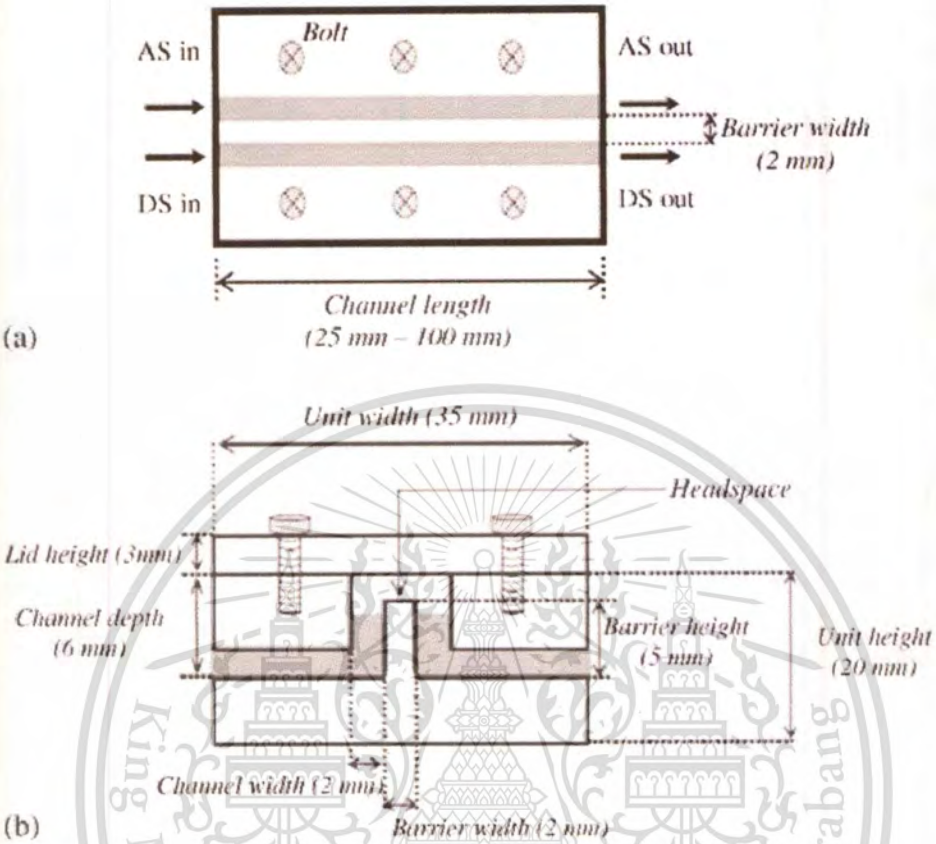

Figure 2.1 Schematic diagram of membraneless gas diffusion unit. (a) Top view; (b) Side view. This picture was taken from [11].

In 2009, a method based on membraneless for the quality control of gasohol was deverloped by S. Muncharoen *et al* [32]. This work applied the membraneless gas diffusion (MBL-GD) deverloped by N. Choengchan (same concept of vaporize unit). The apparatus was slightly modified from our presented by N. Choengchan (Figure 2.2). The analysis was carried out with one-step aqueous extraction of gasohol (1:2 gasohol/water) for determination of ethanol content in gasohol fuel. Detection was based on reduction of dichromate by ethanol vapor with spectrometric detection at 590 nm. This work could determine both gasohol E10 and E20. Detection limit of the technique was 0.9% *(v/v)*.

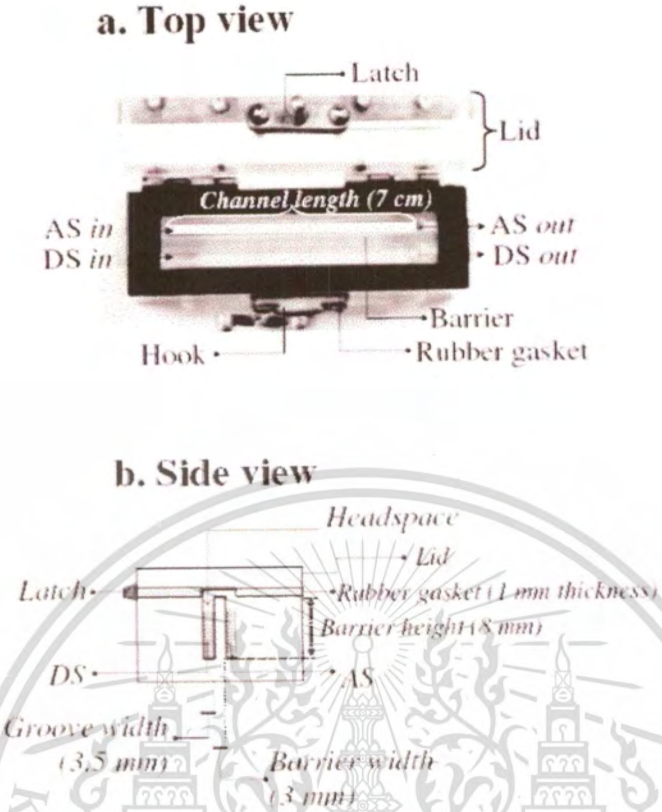

Figure 2.2 The schematic of the membraneless gas-diffusion unit for quantitative analysis of ethanol in gasohol. This picture was taken from [32].

Technique	Separation method	Sample	Analytical performance	Sample throughput	Reference
Membrane					
1). Amperometry and Photometry (oxidation of ABTS as indicatoe)	Polypropylene membrane (Gas diffsion)	Cultivation media	-Working range (0.6 x 10^{-3})-60 % *(v/v)* Ethanol - Linearity range $y = 1.0036x - 0.005$; $r^2 = 0.9992$ - Limit of detection 1 x 10^{-4}% *(v/v)* Ethanol	120-180 samples/h	[33]
2). Amperometry	Porous PTFE membrane (Gas diffusion)	Beer and wine	-Working range 0-15 % *(v/v)* Ethanol - Linearity range $y = 1.0036x - 0.005$; $r^2 = 0.9992$ - Limit of detection 0.0001% *(v/v)* Ethanol	30 samples/h	[34]

Table 2.1 Flow based technique using membrane based and membraneless for quantitative of ethanol in difference types of sample.

3).Photometry, Cr (VI)→ Cr (III) at 600 nm	A Silicon Tubular Membrane (Pervaperation)	Beer, Wine and Sprit	- Working range 0-50 % *(v/v)* Ethanol - Limit of detection 0.5 % *(v/v)* Ethanol	20 samples/h	[35]
4). Photometry, Cr (VI)→ Cr (III) at 600 nm	A semipermeable PTFE membrane (Pervaperation)	Molasses fermentation	- Working range 1-10 %(v/v) Ethanol	20 samples/h	[36]

Table 2.1 Flow based technique using membrane based and membraneless for quantitative of ethanol in difference types of sample.

Technique	Separation method	Sample	Analytical performance	Sample Throughput	Reference
Membraneless					
5). Photometry, Cr (VI)→ Cr (III) at 590 nm	Membraneless gas diffusion unit	Liquors	-Working range 0.5 – 30 % *(v/v)* Ethanol - Linearity range $y = (9.75 \times 10^{-3})x - (1.4 \times 10^{-3})$; $r^2 = 0.999$ - Limit of detection 0.027% *(v/v)* Ethanol	16 samples/h	[10]
(6). Photometry, Cr(VI)→ Cr (III) At 590 nm	Membraneless gas diffusion unit	Fuel (Gasohol)	Method I - Linear range 3 -12 % *(v/v)* Ethanol $Y = (5.6 \times 10^{-2})x (1.14 \times 10^{-2})$;	26 samples/h	[32]

Table 2.1 Flow based technique using membrane and membraneless for quantitative of ethanol in difference types of sample

r^2 = 0.996 Method II - Linear range 3 -80 % *(v/v)* Ethanol Y = (7.72 x 10^{-2}) x (3.80 x10^{-3}); r^2 = 0.996 - Limit of detection 0.09% *(v/v)* Ethanol

Table 2.1 Flow based technique using membrane and membraneless for quantitative of ethanol in difference types of sample

Some of publications of membrane-and membraneless-vaporization with flow based technique are summarized in **Table 2.1**.

In 2007, K. Sereenonchai *et al* [37] presented a new design of membraneless vaporization unit, known as membraneless-vaporization (MBL-VP), for determination of carbonate in supplement tablet. The principle was based on volatilization of carbon dioxide (CO_2) converted from carbonate by reaction with an acid. The detection was done by detecting the change in color of an acid-base indicator (cresol red) at 440 nm. The new unit was composed with four main parts as depicted in Figure 2.3, including (i) acrylic donor holder, (ii) glass donor vial, (iii) silicone gasket (38 mm i.d., 54 mm o.d., 2.0 mm thickness) and (iv) acrylic lid. All the part was locking by stainless steel clasp (Figure 2.3 b). This lock is a fast lock for locking and unlocking.

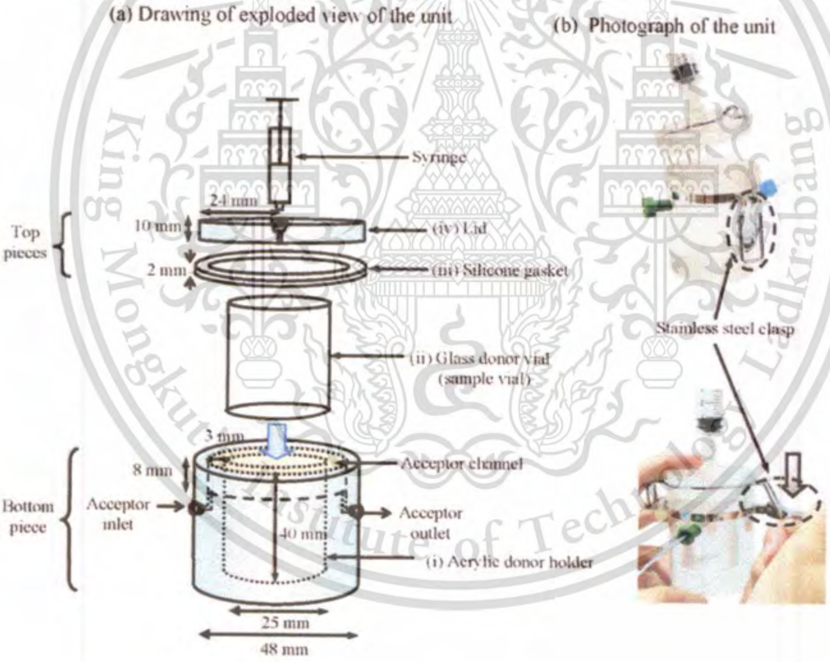
(a) Drawing of exploded view of the unit

(b) Photograph of the unit

(c) Top view of the bottom piece for the 'circular flow' unit

(d) Top view of the bottom piece for the 'semi-circular flow' unit

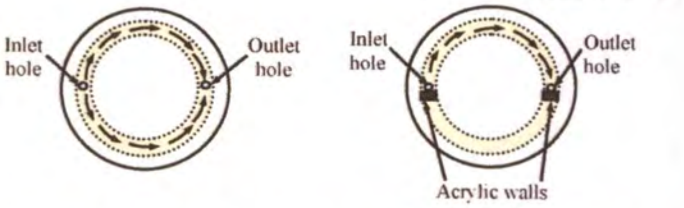

Figure 2.3 (a-d) Schematic diagram and photograph of the membraneless vaporization unit for solid analysis. Note: small arrows in the top views (c and d) represent the flow path. This picture was taken from [37].

In 2009, T. Bhusrisom *et al* [38] proposed a new method for high throughput ethanol analysis, known as microplate vaporization. Microplate vaporization principle was based on membraneless vaporization, a modified 96-well microplate was adopted for simultaneous vaporization of ethanol from the wells containing alcoholic drinks to the wells containing the color forming reagent (Potassium dichromate). An ethanol well and a color forming reagent well were grouped into a pair and separated from each other pairs. The lid was close to start the vaporization of ethanol into color forming reagent. After the lid was taken off, the absorbance of color forming reagents were measured at 590nm by microplate reader.

2.5 CCD in Analytical chemistry

Charge Transfer Devices Photodiode arrays cannot match the performance of photomultiplier tubes in terms of sensitive, dynamic range, and signal-to-noise ratio. Thus, their use has been limited to situations in which the multichannel advantage outweighs their other shortcomings. In contrast, performance characteristics of charge transfer device (CTD) detectors appear to approach those of photomultiplier tubes in addition to having the multichannel advantage. As a consequence, this type of detector is now appearing in ever-increasing numbers in modern spectroscopic instruments. A further advantage of charge transfer detectors is that they are two dimensional in the sense that individual detector elements are arrange in rows and columns. For example, one detector that we describe in the next section consists of 244 rows of detector elements. Each row is made up of 388 detector elements, giving a two-dimensional array of 19,672 individual detectors, or pixels, contained on a silicon chip having dimensions of 6.5 mm by 8.7 mm. With this device, it becomes possible to record an entire two-dimensional spectrum.

Charge transfer detectors operate much like a photographic film in the sense that they integrate signal information as radiation strikes them. There is a cross-sectional depiction of one of the pixels making up a charge transfer array. In this case, the pixel consists of two conductive electrodes overlying an insulating layer of silica. (A pixel in some charge transfer devices is made up of more than two electrodes.) This silica layer separates the electrodes from a region of *n*-doped silicon. This assemble constitutes a metal oxide semiconductor capacitor, which stores the charges formed when radiation strikes the doped silicon. When, as shown, a negative charge is applied to the electrodes, which is energetically favorable for the storage of positive holes. The mobile holes created by the adsorption of protons by the silicon then migrate and collect in this region. (Typically, this region, which is called a potential well, is capable of holding as many as 10^5 to 10^6 charges before overflowing into an adjacent pixel.) In the figure, one electrode is shown as being more negative than the other, making the accumulation of charge under this electrode more favorable. The amount of charge generated during exposure to radiation is measured in either of two ways. In a charge injection device (CID) detector, the voltage change arising from movement of the charge from the region under one electrode to the region under the other is measured. In a charge coupled device (CCD) detector, the charge is moved to a charge-sensing amplifier for measurement.

CCDs and CIDs are appearing in ever-increasing numbers in modern spectroscopic instruments. In spectroscopic applications, charge transfer devices are used in conjunction with multichannel instruments. In addition to spectroscopic applications, charge transfer devices fine widespread applications in solid-state television cameras and microscopy [39].

In 2002, Kompaney-Zareh M., Mansourian M., and Ravaee F. [40] proposed method for colorimetric spot test analysis of Fe (III). Quantitative analysis in this study is based on formation of color spots (points) on a paper and considering the intensity of their color, it's possible to carry out the analysis using a densitometer, like analysis of thin layer chromatography (TLC) data. Several types of densitometers have been reported in the literature; these are expensive devices and include spectrophotometers, CCD cameras and other devices based on the use of CCD arrays. The propose of this work was to design a more cost effective method for spots quantitative analysis through the use of widely available and inexpensive hand-scanner for determining the intensity of color points.

In 2010, L. Lahuerta Zamora, P. Aleman Lopez, G.M. Anton Fos, R. Martín Algarrac, A.M. Mellado Romero,and J. Martínez Calatayud [41] were developed image processing for determination of nickel content in iron meteorite. This method uses imaging analysis to determine nickel with dimethylglyoxime (DMG). The operational procedure involves taking a digital image for a series of standard solutions of the Ni–

DMG complex and one solution of the unknown sample treated in the samemanner as the standards. The image is then processed with suitable software in order to assign a numerical value (analytical signal) to each color spot. Such a value is directly proportional to the analyte concentration in each standard, so it can be used to construct a calibration curve. Interpolating the value for the sample into the calibration curve allows the nickel content of the meteorite to be determined.

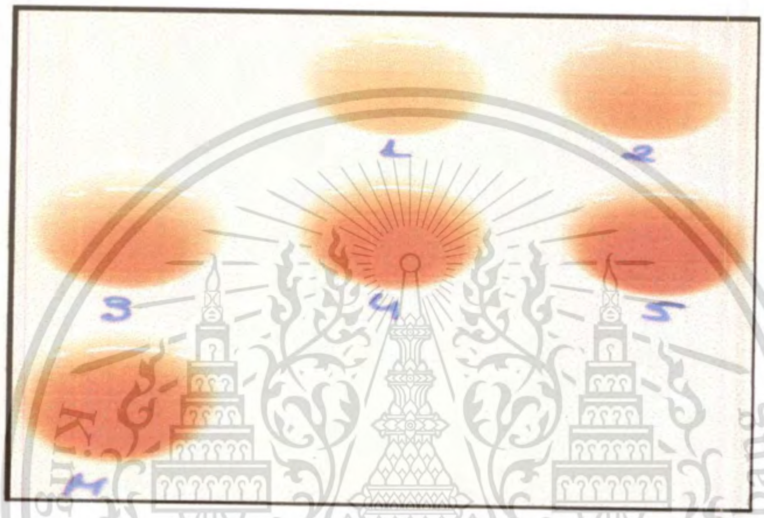

Figure 2.4 Image for the calibration standards (1–5) and sample (M) on the spot plate [41].

CHAPTER III

MATERIALS AND METHODS

This chapter summarizes method for the preparation of standards and chemical as well as the method of analysis.

3.1 Microplate vaporization method

3.1.1 General Instrument

3.1.1.1 Digital camera

A Canon™ Power Shot G12 digital camera was used for capturing image of sample.

3.1.1.2 Analytical balance

A SHIMADZU analytical balance AUX 220 was used for weighting chemicals in the preparation of reagent solutions.

3.1.1.3 Auto micropipette

A Finnpipette® F3 Single Channel Variable and Fixed Volume, Thermo Fisher Scientific Oy (Vantaa, Finland) was used for loading reagent solution into microplate wells.

3.1.1.4 Isotemp oven

An Isotemp Programmable Lab Oven, Fisher Scientific, was used for heating temperature of standard and sample.

3.1.2 Apparatus for Microplate vaporization

3.1.2.1 A modified 96-well plate

A 96 well cell culture plate (Corning, USA) was modified by attaching silicone rubber (8.2 cm x 12.3 cm x 1mm: width x height x depth) onto the plate, as shown in Figure 3.1. This silicone was cut to make 18 rectangular holes to provide head spaces above the 18 pairs of wells. The rest of the wells in the microplate were not used in the vaporization and were sealed under the silicone after attaching the cut-silicone with the plate.

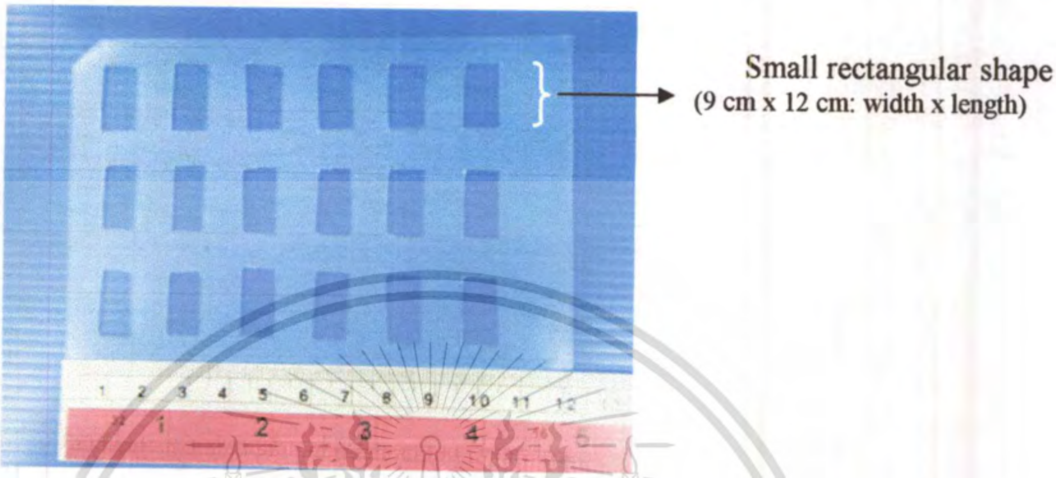

Figure 3.1 The photograph of the silicone gasket (Top View).

3.1.2.2 A home- made cover box

The purpose of cover box is to eliminate the external scattering light source which can disturb the experiment. This box made of a paper box (21.5cm x 30.8cm x 48cm: width x height x depth) and painted inside and outside with black. This box has a hole (7cm diameter) for inserting camera lens. Schematic diagram and photo of the box are illustrated in Figure 3.2.

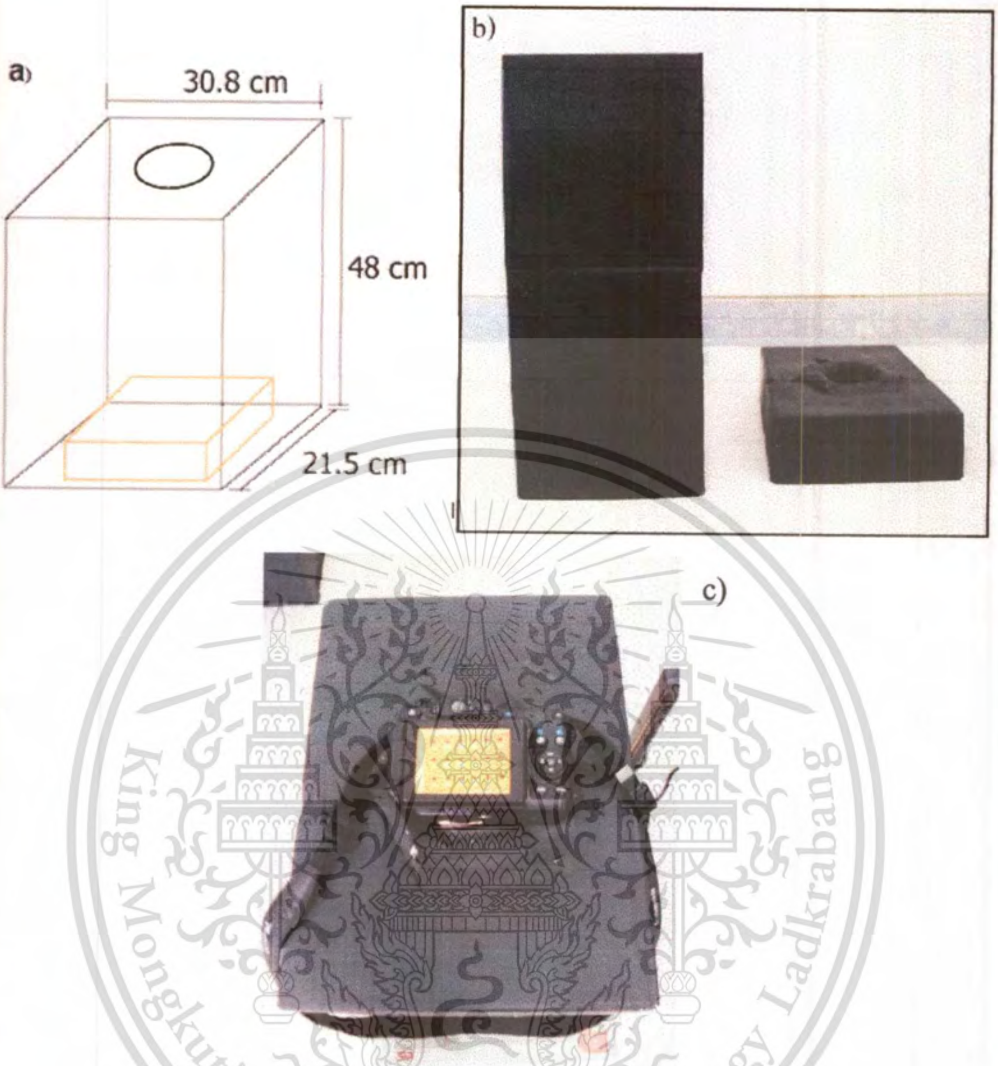

Figure 3.2 a) Drawing of home-made cover box with projector as a light source
b) Photograph of home-made cover box
c) Using of home-made cover box in image processing

3.1.3 Reagents

All chemicals used in this work were analytical reagent (AR) grade. Deionized-distilled water (18.2 mΩ cm^{-1}), obtained from a Milli-Q- system, and was used for preparation of reagent solutions. List of chemicals and their suppliers are summarized in Table 3.1.

Table 3.1 List of chemicals and their suppliers

Chemical	Formula	Supplier
Potassium dichromate	$K_2Cr_2O_7$	CARLO ERBA reagents
Sulfuric acid	H_2SO_4	THOMAS BAKER chemicals
Ethanol	C_2H_5OH	CARLO ERBA reagents

3.1.4 Preparation of Reagent, Standard Solution and Sample

3.1.4.1 Acidic dichromate solution

Potassium dichromate crystal (A.R. grade., CARLO ERBA reagents) was dissolved 0.2940g in 10.00 mL of deionized- distilled water (D.I. water) and slowly adding 14 mL of conc. H_2SO_4 (98 % A.R. grade., THOMAS BAKER chemicals). The solution was finally made to 100 mL with D.I. water.

3.1.4.2 Standard ethanol solution

Working standard solution were freshly prepared by suitable dilution of 99.9 % *(v/v)* ethanol (Merck , Germany) with D.I. water in order to make 5, 10, 20, 30, and 40 % (v/v) ethanol solution.

3.1.4.3 Sample preparation

All of the alcoholic beverages were purchased from local markets and department stores. They were all made by Thai manufacturers samples were utilized as produced by the manufacturer without any preparation.

3.1.5 Procedure

3.1.5.1 Optimization

(a) Effect of heating temperature

The effect of heating temperature was investigated in the range from room temperature to 90 °C. The concentration of $K_2Cr_2O_7$ and H_2SO_4 were kept at 0.1 mol L^{-1} and 2.5 mol L^{-1}, respectively. The concentration of standard ethanol was used from 0 to 40 % *(v/v)*. The microplate was covered with the lid for 7 min. Then, the lid was taken off and the digital camera was need for capturing images at the similar time by placed on the projector with home-made cover box at 30 sec after taken out of the oven. Finally, we used Image J program to measure intensity of images. Results are discussed in Section 4.2.1.

(b) Effect of diffusion time

Diffusion time is defined as the interval time since the plate was taken in the oven until the plate was taken off the oven. The diffusion time was varied from 3 to 10 min. 300 μL of 0.1 mol L^{-1} $K_2Cr_2O_7$ in 2.5 mol L^{-1} H_2SO_4 was pipetted into reagent well and 300 μL of standards ethanol (0 to 40 %*(v/v)*) were pipetted into sample/standard wells. After reaching the desired diffusion time, the lid was taken off and placed on the projector with home-made cover box. Then turn on light of the projector and used digital camera for capturing images at 30 sec after taken out of the oven. Finally, Image J program was exploited to measure intensity of images. Results are discussed in Section 4.2.2

(c) Effect of concentration of reagents

In this work, dichromate in sulfuric acid medium was used as scrubbing reagent. Influence of the concentrations of dichromate and sulfuric acid were examined independently. Investigated concentration was ranging from 0.01 to 1.0 mol L^{-1} and 1.5 to 3.0 mol L^{-1} for dichromate and sulfuric acid, respectively. The employed volume of standard and reagent were 300 μL each. The diffusion time was fixed at 7 minutes. Then, the lid was taken off and the digital camera was need for capturing images at the similar time by placed on the projector with home-made cover box at 30 sec after taken out of the oven. Finally, Image J program was exploited to measure intensity of images. Results are discussed in Section 4.2.3.

(d) Effect of camera condition

For the effect of camera, we choose to fixed aperture size in order to obtain the most stabilized image. Hence we will vary shutter speed and this will result in the brightness of our images. The range of shutter speed was varied to make exposure value become 2, 1, 0, -1 and -2 (light to dark image). 300 μL of 0.1 mol L^{-1} $K_2Cr_2O_7$ in 2.5 mol L^{-1} H_2SO_4 was pipetted into reagent well and 300 μL of standards ethanol (0 to 40% *(v/v)*) were pipetted into sample/standard wells. The diffusion time was fixed at 7 minutes. Then, the lid was taken off and the digital camera was need for capturing images at the similar time by placed on the projector with home-made cover box at 30 sec after taken out of the oven. Finally, Image J program was exploited to measure intensity of images. Results are discussed in Section 4.2.4.1. Another experiment was done to investigate the effect of ISO by fixed aperture size at f4.5 and exposure at 0. Results are discussed in Section 4.2.4.2.

3.1.5.2 Analytical performance

(a) Precision

Precision is determined by the following formula.

$$RSD = \frac{SD}{\bar{x}} \times 100$$

Eighteen standard 10% (v/v) of ethanol were measured for their intensity by using condition in Table4.1. This was done by five replicates in order to obtain both RSD within well and RSD between wells. Results are discussed in Section 4.3.1.1 and 4.3.1.2.

(b) Limit of detection

Twelve blanks were analyzed for the limit of detection by using condition in Table 4.1.

Limit of detection is determined by this formula.

$$LOD = \frac{3SD_{Blank}}{Slope}$$

Results discussed in section 4.3.2.

(c) Accuracy

Accuracy was studied by evaluation on analytical recovery.

Recovery can be calculated according to the following equation:

$$\%Recovery = \frac{[Spiked\ sample] - [Sample]}{[Standard]} \times 100$$

Where: [Spiked sample] = [Sample + Standard]

[Sample] = [Sample + D.I. water]

[Standard] = [D.I. water + Standard]

Addition of 10 mL of standard ethanol (30% *v/v*) into eight alcoholic beverage samples and synthetic samples were carried out. The spiked samples were then analyzed using the condition described in Table 4.1. Results are discussed in Section 4.3.3

3.1.5.3 Application to alcoholic beverages and validation

Seven samples of alcoholic beverage, form section 3.1.5.2 can be used to calculated amount of ethanol from sample's bottle. Then these values will be used to compare with label values. Results are discussed in section 4.3.4.

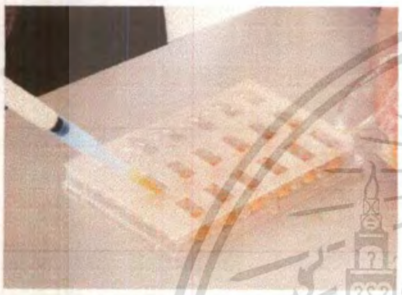

Pipette reagents and samples into wells by using micropipette. This takes 2 minutes

Close the lid. After 30 seconds microplate was put into oven at 70°C for 7 minutes.

Take a microplate out and then put into cover box. 30 seconds later take a photo.

Wash and dry microplate to be ready for using again for 5 minutes

Total time per cycle 15 minutes

Figure 3.2 Flow chart for image processing

CHAPTER IV
RESULTS AND DISCUSSION

This chapter explains the modified tools for microplate vaporization method and optimization of the method for ethanol analysis in alcoholic beverage. Detection was based on a colorimetric method with image processing.

The colorimetric reaction was based on the reaction between ethanol and acidic dichromate. Reduction of potassium dichromate (VI) to chromium (III), yielding Cr^{3+}(aq) was monitored at 590 nm (equation).

$$3C_2H_2OH_{(aq)} + 2Cr_2O_7^{2-}{}_{(aq)} + 16H^+{}_{(aq)} \rightarrow 3CH_3COOH_{(aq)} + 4Cr^{3+}{}_{(aq)} + 11H_2O_{(l)} \qquad \ldots(2)$$

(Orange) (Green)

Here, we observe the intensities of color change while the reaction is proceeding. The more ethanol the greater change in the intensities. The change in reds intensity will be observes, since the color of reagent is change from orange to green (thus the reds intensity is decrease). The intensity can be measured as numerical number using software called Image_J. Calibration curve is based on linear relation between reflectance of red color and amount of ethanol.

The reflectance can be calculated using the following equation [39]

$$R_x = -\log [I_x/I_{x,w}] \qquad \ldots (3)$$

in which R = reflectance

x = color channel (red, greed, or blue)

w = white (blank)

4.1 Quantitation method for color intensity

By [39] the authors used the mean reflectance of three color channel (red, green, and blue). Hence equation (3) was used for all three color channel to calculate their reflectance. However, it was observed by our research that the mean reflectance gave poor linearity relation, and also poor sensitivity (slope of calibration curve). The result is shown in Figure 4.1.

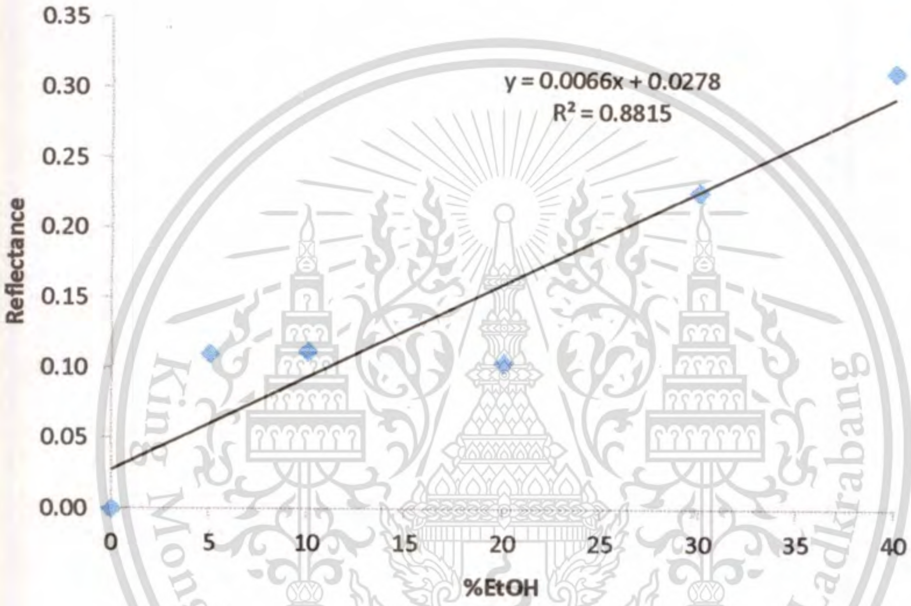

Figure 4.1 Mean reflectance vs. %EtOH

Therefore we divided the mean reflectance into three color reflectance. Figure 4.2 (A), (B), and (C) show the relation between reflectance and percentage of ethanol in red, green, and blue channel, respectively. Here the reflectance of red channel gave the best sensitivity and linearity. This can be explained by the change in color of our reagents from orange to green. Actually if the reaction was complete, the color would be green- blue color. But the condition that we deployed was may be uncompleted reaction, so some parts of reagent were changed into green while some were not. Therefore, green and blue colors were negliglible. Only definitely change is the red color because even blue or green change or not, red is always decreasing.

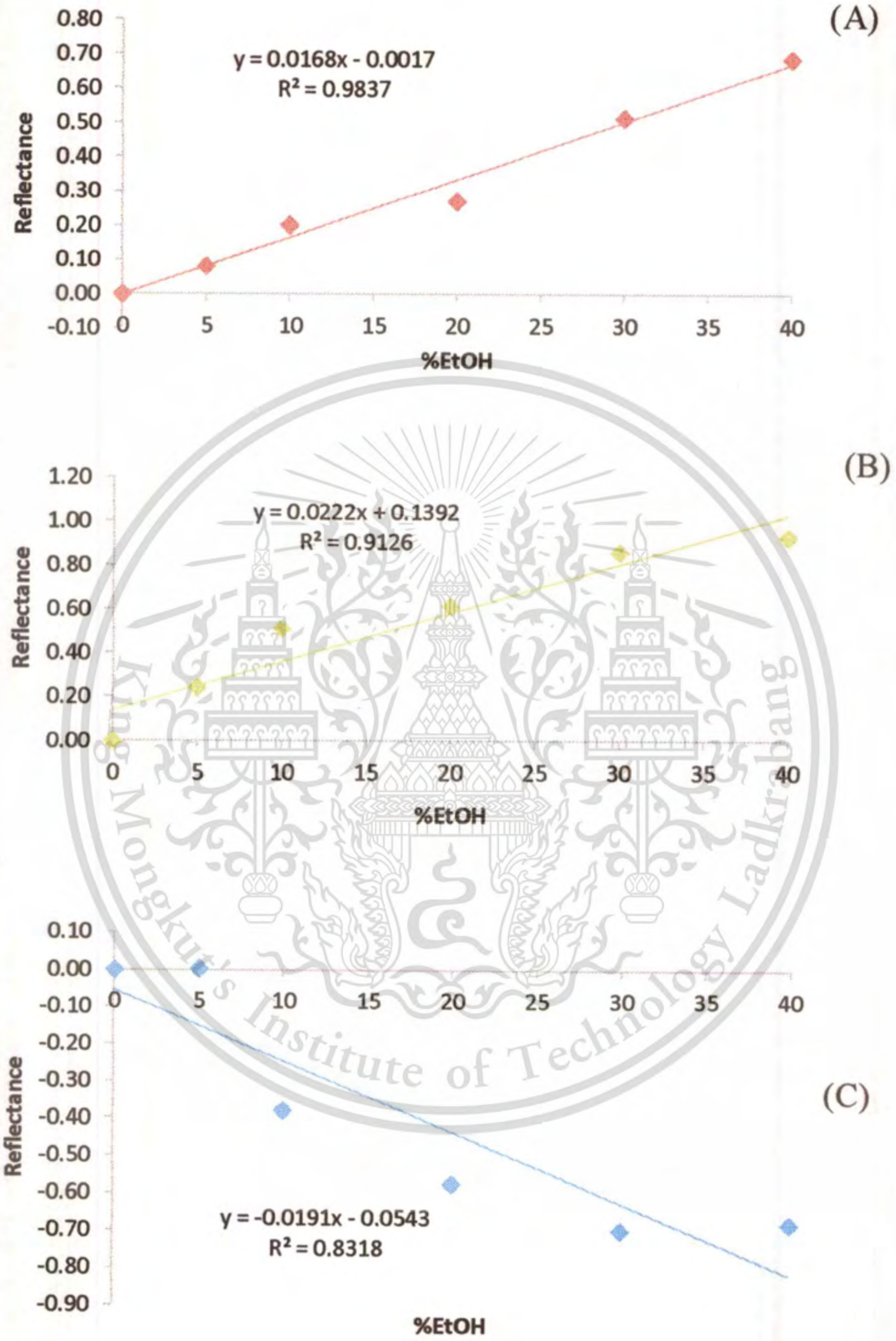

Figure 4.2 (A) Reflectance of red vs. %EtOH (B) Reflectance of green vs. %EtOH (C) Reflectance of blue vs. %EtOH

4.2. Optimization

4.2.1. Effect of temperature

Figure 4.3 (A) and (B) present effect of temperature on sensitivity of our method. When temperature is increased, the higher sensitivity will get due to the increased temperature accelerates the rate of diffusion time and chemical reactions which make the reagent color changed more clearly but when the temperature is risen up more than 70°c, microplate will be distorted.

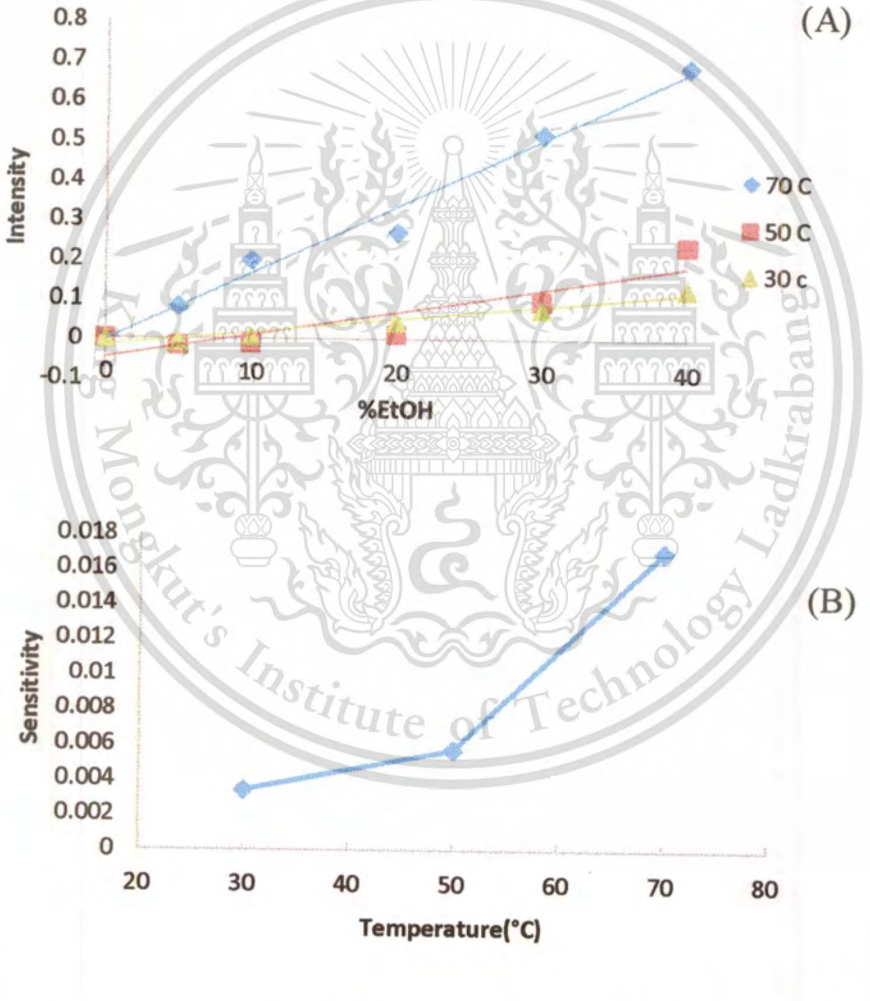

Figure 4.3 Effect of temperature on sensitivity. Reagent 300 µL 0.1 mol L^{-1} $K_2Cr_2O_7$ in 2.5 mol L^{-1} H_2SO_4. Diffusion time is 7 minutes. (A) Intensity vs. %Ethanol (B) Sensitivity vs. Temperature

4.2.2 Effect of diffusion time

Figure 4.4 (A) and (B) present effect of diffusion time on sensitivity. The increased diffusion time has affected on a growth of sensitivity owing to the diffusion range of Ethanol into reagent wells are longer which has the result in clearly changing of reagent color. In this case, diffusion time at 7 minutes is selected because the shortest analysis time is required.

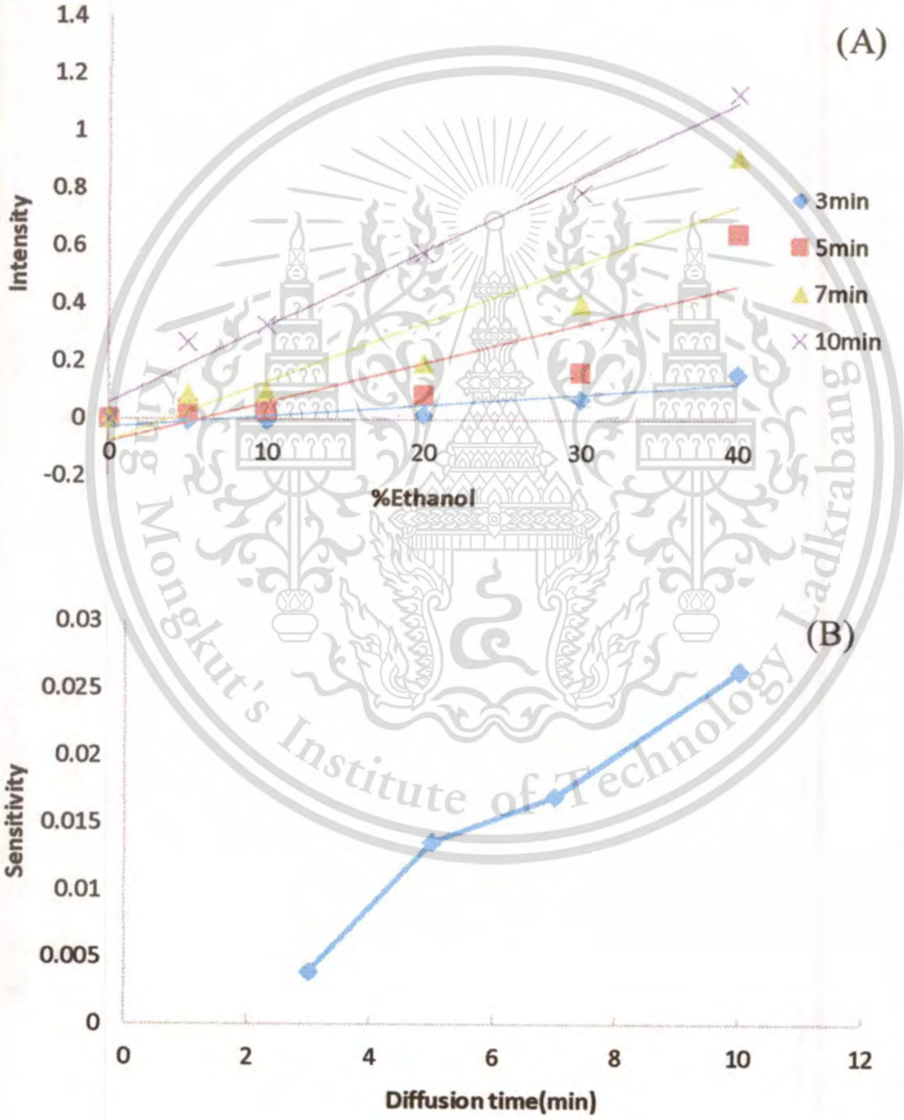

Figure 4.4 Effect of diffusion time on sensitivity. 300 µL 0.1 mol L^{-1} $K_2Cr_2O_7$ in 2.5 mol L^{-1} H_2SO_4. Temperature is 70 °C (A) Intensity vs. %Ethanol (B) Sensitivity vs. Diffusion time

4.2.3 Effect of concentration of reagents

Figure 4.5 (A), (B) and 4.6 (A), (B) illustrate effect of dichromate and sulfuric acid concentration respectively.

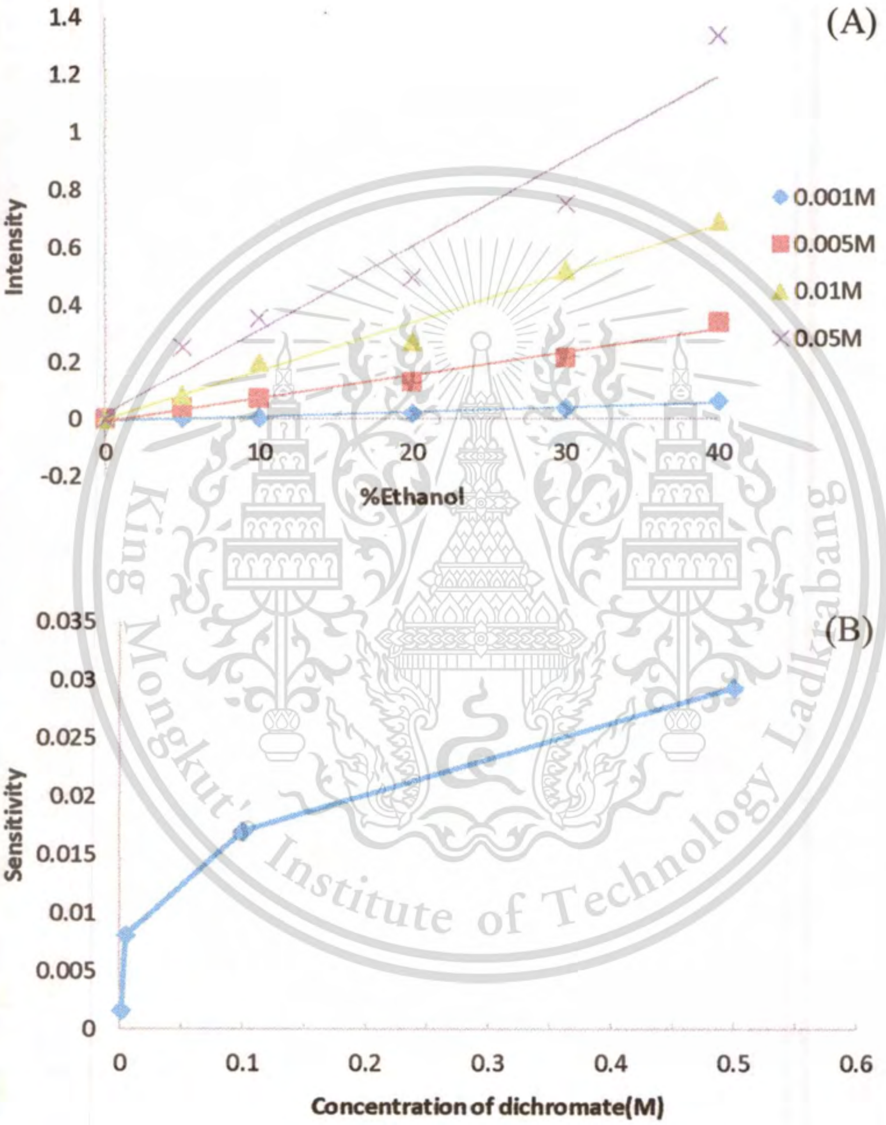

Figure 4.5 Effect of dichromate concentration. Temperature is 70 °C. Diffusion time is 7 minutes. Concentration of sulfuric acid is 2.5M. (A) Intensity vs. %Ethanol (B) Sensitivity vs. Concentration of dichromate

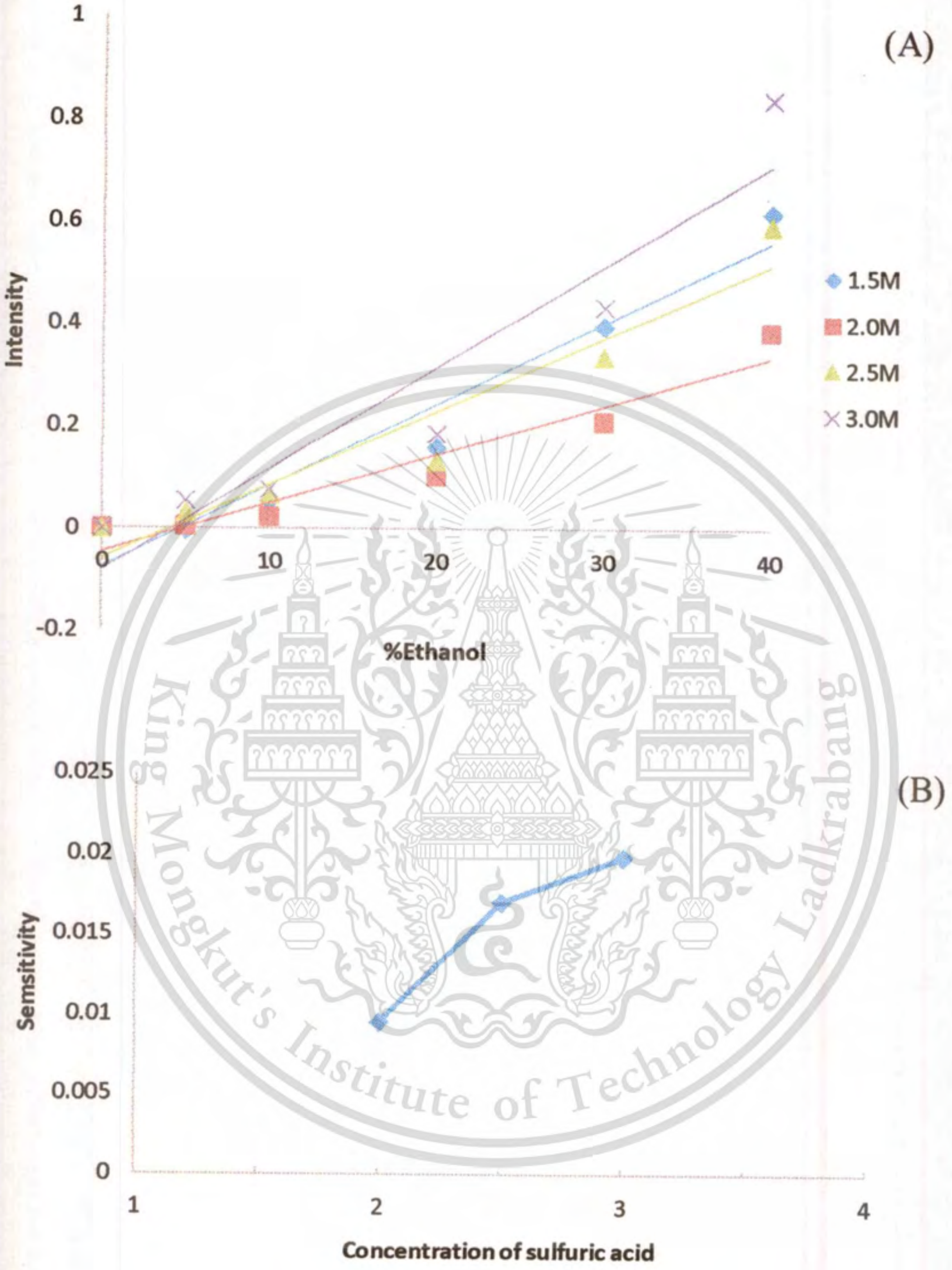

Figure 4.6 Effect of sulfuric acid concentration. Temperature is 70 °C. Diffusion time is 7 minutes. Concentration of dichromate is 0.1 M. (A) Intensity vs. %Ethanol (B) Sensitivity vs. Concentration of sulfuric acid

Actually the color of reagent is from Potassium dichromate so when the concentration of Potassium dichromate is increased, the sensitivity will be increased and can be observed more easily. In this research, the concentration of Potassium dichromate is 0.1M since it doesn't over consume. The high concentration is more difficult in solubility of reagent. (1M. Potassium dichromate which is insoluble has no effect. Solubility of dichromate 10.5%(w/w) at 20 °C [42]).

Ability in splitting of Potassium dichromate in Sulfuric is better, the color can be observed more clearly so the higher concentration of sulfuric can improve and increases the sensitivity. The chosen concentration of Sulfuric is 2.5M because of the consumption and dangerous of sulfuric acid.

4.2.4 Effect of camera effect

For the effect of camera we studied effect of shutter speed and ISO. The effect of aperture size will not be investigated because we need the largest aperture size to provide the fastest shutter speed in order to give the most stable image

4.2.4.1 Effect of brightness (exposure value)

Figure 4.7 (A) and (B) present effect of brightness on sensitivity. Brightness is represented by the exposure value. The higher exposure value means the brighter image. Here the darker image results in the higher sensitivity. This effect can be explained by when you looking in the dark the change in color is more obviously than in the bright. Hence we select the exposure value at -2.

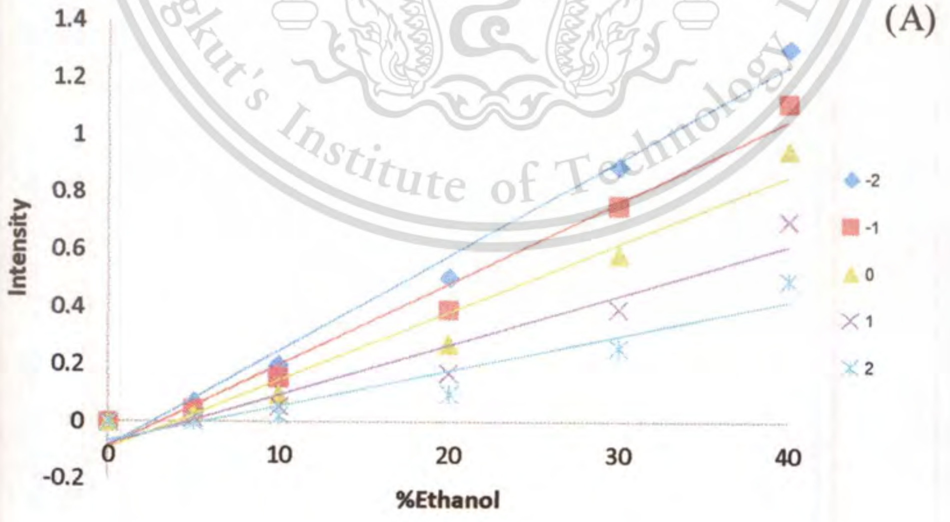

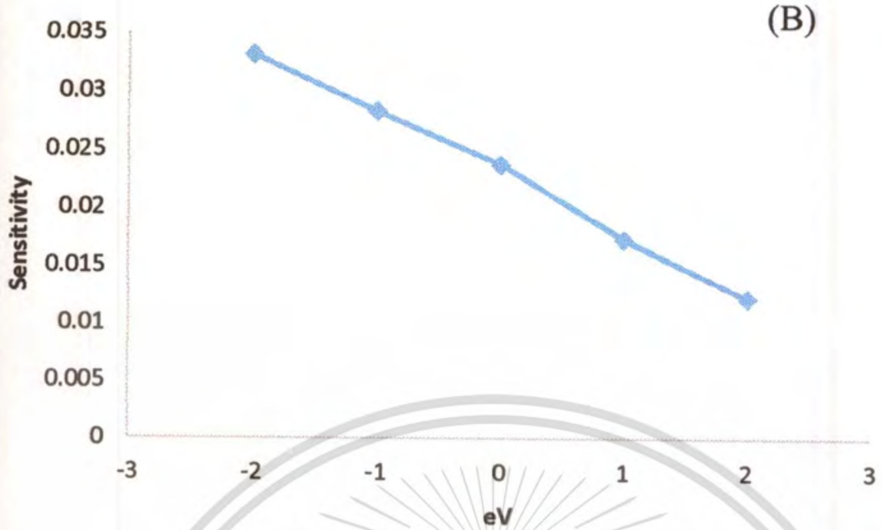

Figure 4.7 Effect of speed shutter on sensitivity. Reagent 300 µL 0.1 mol L^{-1} $K_2Cr_2O_7$ in 2.5 mol L^{-1} H_2SO_4. Diffusion time is 7 minutes. Temperature is 70 °C. (A) Intensity vs. %Ethanol (B) Sensitivity vs. exposure value.

4.2.4.2 Effect of ISO

Figure 4.8 presents effect of ISO on sensitivity. ISO means the sensitivity to light of camera's sensor (CCD). Increasing ISO result in the brighter image (hence we can use higher shutter speed) and noise in our image. From our result ISO has no effect on sensitivity. In this research we select ISO at 100 because of comfortable for using old camera (in old camera high ISO value can cause noise in image easier than in newer camera)

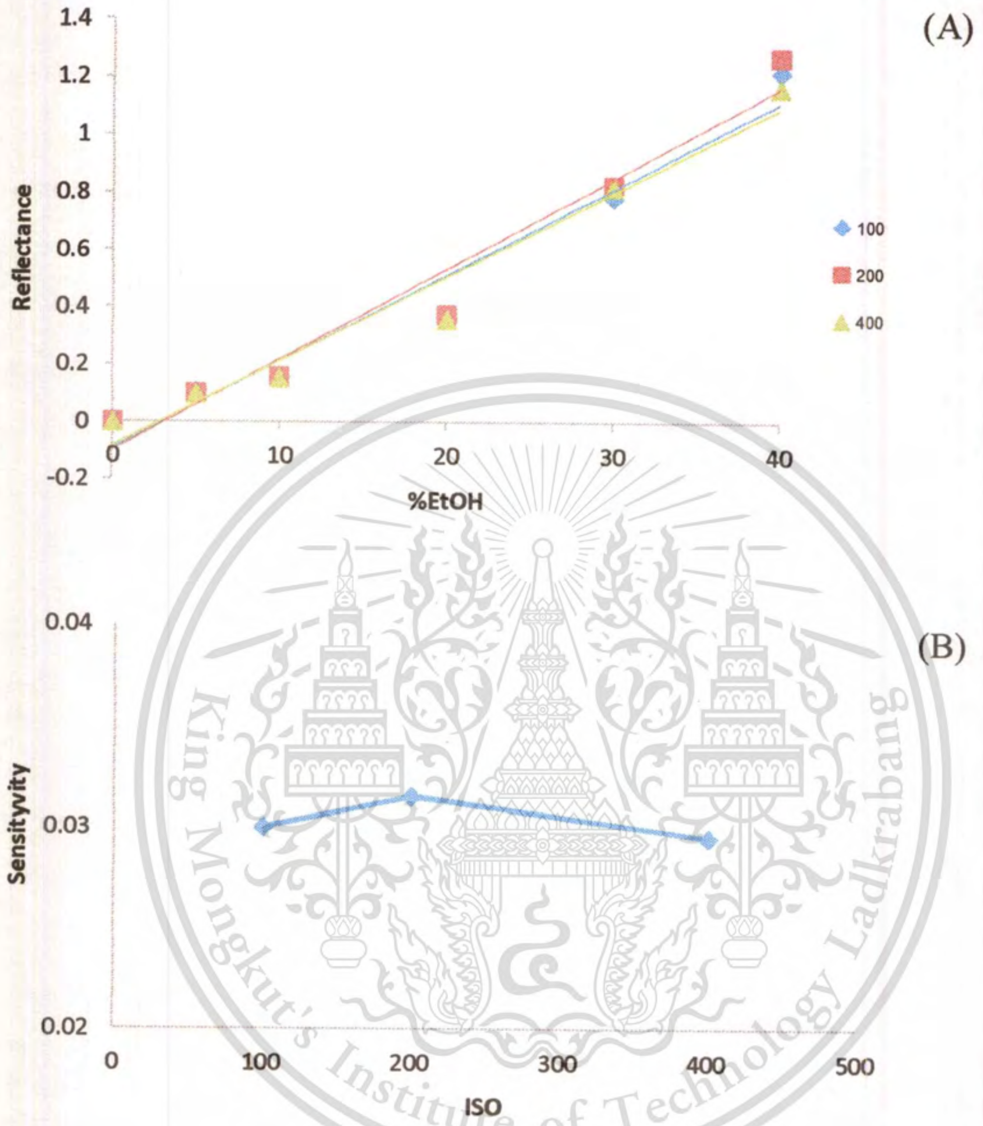

Figure 4.8 Effect of speed ISO on sensitivity. Reagent 300 μL 0.1 mol L^{-1} $K_2Cr_2O_7$ in 2.5 mol L^{-1} H_2SO_4. Diffusion time is 7 minutes. Temperature is 70 °C. (A)Intensity vs. %Ethanol (B) Sensitivity vs. ISO

4.2.5 An optimal condition

Study range and selected value as an optimal condition are summarized in Table4.1

Table 4.1 Studied and selected parameters for an optimization condition for determination of ethanol by microplate vaporization device

Parameter	Studied range	Selected value
Temperature (°C)	25-70	70
Diffusion time (min)	3-10	7
Dichromate concentration (mol L^{-1})	0.01-0.5	0.1
Sulfuric acid concentration (mol L^{-1})	2.0-3.0	2.0
Exposure(eV)	(-2)-(+2)	-2
ISO	100-400	100

4.3 Analytical performance

4.3.1 Precision

Precision in this analysis is represented by RSD value of intensity. The smaller RSD mean the higher precision for this analysis. This can be done by five replicates of eighteen wells of standard 10% (v/v) of ethanol.

4.3.1.1 Precision between wells

The result of five RSD value from each replicates shows that the precision between wells is low (Table4.2 shows result of RSD between well). These RSD calculated from intensity of eighteen standard 10 % (v/v) of ethanol of each replicates.

Table 4.2 RSD between well

Replicate	RSD
1	48.34
2	36.90
3	28.47
4	29.63
5	42.07

4.3.1.2 Precision within well

Intensities of the same well were measured for five replicates. This were done for eighteen well of standard 10 % (v/v) ethanol. Table4.3 shows the result form RSD within well.

Table4.3 RDS within well

Well	RSD	Well	RSD
1	49.73	10	24.86
2	39.14	11	16.81
3	7.70	12	43.00
4	6.22	13	61.04
5	20.15	14	47.03
6	61.42	15	36.79
7	35.26	16	40.47
8	45.27	17	56.89
9	24.70	18	15.80

4.3.2 Limit of detection

Detection limit (3SD) is 1.99% *(v/v)* ethanol. Which mean the method cannot detect very small amount of ethanol.

4.3.3 Analytical time

With in 1 hour, there were 72 samples can be analyzed.

4.3.4 Accuracy

Accuracy of our proposed method can be determined from recovery study. The recoveries of all samples give the satisfied results. However in some wells color change are different. The results of recovery study are summarized in Table 4.4

Table4.4 Results of recovery study

Sample	**Ethanol content (% *v/v*, mean ± SD)**			**Recovery(%)**
	Original*	**Added**	**Founded***	
Thai beer	6.62	12	18.89	102.25
Sparking Thai wine	5.36	12	17.24	99
Thai liquor 1	12.52	12	24.94	103.5
Thai liquor 2	15.22	12	28.09	107.25
Scotch Whiskey	20.89	12	33.52	105.25
Thai-herb juice 1	3.69	12	15.25	96.33
Thai-herb juice 2	6.04	12	19.23	109.92
Thai-herb juice 3	4.92	12	16.23	94.25

* See Appendix H for raw data.

Table4.5 Summary of analytical performance of microplate vaporization with image processing for ethanol analysis

Performances	**Values**
Linear working range	5 to 40 %(v/v) ethanol
Calibration equation	$y = (0.0346 \pm 0.0057)x - (0.1144 \pm 0.0844)$
Limit of detection (3SD)	1.99% (v/v) ethanol
Precision between well	24.98%
Analysis time	72 sample per plate per hour 15 minutes per cycle

4.3.5 Application to alcoholic beverages and validation

To prove the reliability of the proposed method, the method was applied to quantitative determination of ethanol in commercial alcoholic beverage samples. Comparison of ethanol contents, determined by the proposed method with the labeled value is shown in Table 4.6.

Table 4.6 Comparison of ethanol concentration in alcoholic beverage which were determined by the labeled

Sample	% (v/v) of ethanol	
	Labeled	**Obtain***
Thai beer	5	8.27 ± 1.62
Sparking Thai wine	5	6.72 ± 2.38
Thai liquor 1	15	22.06 ± 5.43
Thai liquor 2	28	25.22 ± 6.26
Scotch Whiskey	40	34.97 ± 10.29
Thai-herb juice 1	0	4.61 ± 1.22
Thai-herb juice 2	0	7.55 ± 0.61
Thai-herb juice 3	0	6.39 ± 0.78

---

* See Appendix H for raw data.

CHAPTER V

CONCLUSION

5.1 Microplate vaporization with image processing method was developed for detection /determination of ethanol.

5.2 The advantages and disadvantages of microplate vaporization with image processing are summarized as the following

5.2.1 Advantages of microplate vaporization with image processing

(i) Suitable for routine for laboratory work due to rapid determination (72 samples per hour see Table 4.5)

(ii) Cost saving apparatus compare with previous methods.

(iii) Minimizing reagent consumption and waste production.

5.2.2 Disadvantages of microplate vaporization with image processing

(i) Poor precision of the method (high value of RSD between wells and RSD within well)

5.3 Suggestion for further development

The reason for poor analytical performance comes from the poor distribution of heat in the oven. The benefits of heat are to accelerate the rate of diffusion and reaction. The poor heat distribution can cause different in temperature of each wells. Therefore the poor heat distribution can result in unequally reaction rate between pairs of wells.

Another reason might come from the leakage of the lid. The lid is not heavy enough to completely cover microplate. Therefore our system (pair of sample and reagent wells) is not close system. This can cause negative effect to our result for example leakage of ethanol into another pair of well or leakage of ethanol to atmosphere.

5.4 Possibility study on determination of acetaldehyde

Acetaldehyde is another volatile compound which can be found in alcoholic beverages. Amount of acetaldehyde in beverages have to be concerned because of its harmful characteristic. Acetaldehyde can also have a colorimetric reaction like ethanol but with different reagent. The reagent which will be deployed is mixed reagents of sodium nitroprusside and morpholine. In this research we have applied an optimal condition in ethanol analysis to acetaldehyde analysis, but we failed. Hence if we can analyze both ethanol and acetaldehyde by using the same condition, we shall reduce a lot of analysis time to analyze both of them.

REFERENCES

1. Alcoholic beverages-Wikipedia, http://en.wikipedia.org/wiki/Alcoholic_beverage.

2. Facts_and_Figures_ch3.pdf (application/pdf Object). http://www.searo.who.int/LinkFiles/Facts_and_Figures_ch3.pdf.

3. Zeikus, J. G., Chemical and fuel production by anaerobic bacteria. *Annu Rev Microbiol* **1980,** *34*, 423-64.

4. Dombek, K. M.; Ingram, L. O., Ethanol production during batch fermentation with Saccharomyces cerevisiae: changes in glycolytic enzymes and internal pH. *Appl Environ Microbiol* **1987,** *53* (6), 1286-91.

5. Sobocan, G.; Glavic, P., Optimization of ethanol fermentation process design. *Applied Thermal Engineering* **2000,** *20* (6), 529-543.

6.องค์การสุรากรมสรรพสามิตกระทรวงการคลัง-กระบวนการผลิตแอลกอฮอล์. http://www.liquor.or.th/main/index.php?option=com_content&task=view&id=86&Itemid=28&lang=en.

7. The Cornish Cyder Farm, home of the Cornish Scrumpy Co. Cider Brandy Farmhouse Cider. http://www.thecornishcyderfarm.co.uk/museum.htm.

8. พระราชกิจจานุเบกษา, พระราชบัญญัติมาตรฐานผลิตภัณฑ์อุตสาหกรรมไวน์. **2544.**

9. พระราชกิจจานุเบกษา, พระราชบัญญัติมาตรฐานผลิตภัณฑ์อุตสาหกรรมสุรากลั่น. **2544.**

10. Charge-coupled device http://en.wikipedia.org/wiki/Charge-coupled_device

11. Choengchan, N.; Mantim, T.; Wilairat, P.; Dasgupta, P. K.; Motomizu, S.; Nacapricha, D., A membraneless gas diffusion unit: Design and its application to determination of ethanol in liquors by spectrophotometric low injection. *Analytica Chimica Acta* **2006,** *579* (1), 33-37.

12. AOAC, A. O. A. C., *Official methods of the association of official analytical chemists*. Verginia, 1990; Vol. 2, p 961-964, 739-741.

13. Wang, M. L.; Choong, Y. M.; Su, N. W.; Lee, M. H., A rapid method for determination of ethanol in alcoholic beverages using capillary gas chromatography. *Journal of Food and Drug Analysis* **2003,** *11* (2), 133-140.

14. Wang, M. L.; Wang, J. T.; Choong, Y. M., Simultaneous quantification of methanol and ethanol in alcoholic beverage using a rapid gas chromatographic method coupling with dual internal standards. *Food Chemistry* **2004,** *86* (4), 609-615.

15. Li, H. L.; Chai, X. S.; Deng, Y. L.; Zhan, H. Y.; Fu, S. Y., Rapid determination of ethanol in fermentation liquor by full evaporation headspace gas chromatography. *Journal of Chromatography A* **2009,** *1216* (1), 169-172.

16. Yarita, T.; Nakajima, R.; Otsuka, S.; Ihara, T.; Takatsu, A.; Shibukawa, M., Determination of ethanol in alcoholic beverages by high-performance liquid chromatography-flame ionization detection using pure water as mobile phase. *Journal of Chromatography A* **2002,** *976* (1-2), 387-391.

17. Endelmann, A.; Diewok, J.; Baena, J. R.; Lendl, B., High-performance liquid chromatography with diamond ATR-FTIR detection for the determination of carbohydrates, alcohols and organic acids in red wine. *Analytical and Bioanalytical Chemistry* **2003,** *376* (1), 92-97.

18. Vonach, R.; Lendl, B.; Kellner, R., High-performance liquid chromatography with real-time Fourier-transform infrared detection for the determination of carbohydrates, alcohols and organic acids in wines. *Journal of Chromatography A* **1998,** *824* (2), 159-167.

19. Lvova, L.; Paolesse, R.; Di Natale, C.; D'Amico, A., Detection of alcohols in beverages: An application of porphyrin-based Electronic tongue. *Sensors and Actuators B-Chemical* **2006,** *118* (1-2), 439-447.

20. Santos, A. S.; Pereira, A. C.; Duran, N.; Kubota, L. T., Amperometric biosensor for ethanol based on co-immobilization of alcohol dehydrogenase and Meldola's Blue on multi-wall carbon nanotube. *Electrochimica Acta* **2006,** *52* (1), 215-220.

21. Gouveia-Caridade, C.; Pauliukaite, R.; Brett, C. M. A., Development of electrochemical oxidase biosensors based on carbon nanotube-modified carbon film electrodes for glucose and ethanol. *Electrochimica Acta* **2008,** *53* (23), 6732-6739.

22. Mizgunova, U.; Zolotova, G.; Dolmanova, I., Enzymic method for the determination of ethanol and methanol with spectrophotometric detection of the rate of the process. *The Analyst* **1996,** *121* (4), 431-433.

23. Gallignani, M.; Ayala, C.; Brunetto, M. D.; Burguera, J. L.; Burguera, M., A simple strategy for determining ethanol in all types of alcoholic beverages based on its

on-line liquid-liquid extraction with chloroform, using a flow injection system and Fourier transform infrared spectrometric detection in the mid-IR. *Talanta* **2005,** *68* (2), 470-479.

24. Magrí, A. D.; Magrí, A. L.; Balestrieri, F.; Sacchini, A.; Marini, D., Spectrophotometric micro-method for the determination of ethanol in commercial beverages. *Fresenius' Journal of Analytical Chemistry* **1997,** *357* (7), 985-988.

25. Seo, H.-B.; Kim, H.-J.; Lee, O.-K.; Ha, J.-H.; Lee, H.-Y.; Jung, K.-H., Measurement of ethanol concentration using solvent extraction and dichromate oxidation and its application to bioethanol production process. *Journal of Industrial Microbiology and Biotechnology* **2009,** *36* (2), 285-292.

26. Tipparat, P.; Lapanantnoppakhun, S.; Jakmunee, J.; Grudpan, K., Determination of ethanol in liquor by near-infrared spectrophotometry with flow injection. *Talanta* **2001,** *53* (6), 1199-1204.

27. Fletcher, P. J.; van Staden, J. F., Determination of ethanol in distilled liquors using sequential injection analysis with spectrophotometric detection. *Analytica Chimica Acta* **2003,** *499* (1-2), 123-128.

28. Borges, S. S.; Frizzarin, R. M.; Reis, B. F., An automatic flow injection analysis procedure for photometric determination of ethanol in red wine without using a chromogenic reagent. *Analytical and Bioanalytical Chemistry* **2006,** *385* (1), 197-202.

29. Pascoa, R. N. M. J.; Vidigal, S. S. M. P.; Toth, I. V.; Rangel, A. O. S. S., Sequential injection system for the enzymatic determination of ethanol in wine. *Journal of Agricultural and Food Chemistry* **2006,** *54* (1), 19-23.

30. Vidigal, S.; T th, I.; Rangel, A., Sequential injection-LOV format for peak height and kinetic measurement modes in the spectrophotometric enzymatic determination of ethanol: Application to different alcoholic beverages. *Talanta* **2008,** *77* (2), 494-499.

31. Lei, L.; Mattos, I. L.; Chen, Y., Microfluidic devices for optical determination of ethanol concentration. *Microelectronic Engineering* **2008,** *85* (5-6), 1318-1320.

32. Muncharoen, S.; Sitanurak, J.; Tiyapongpattana, W.; Choengchan, N.; Ratanawimarnwong, N.; Motomizu, S.; Wilairat, P.; Nacapricha, D., Quality control of gasohol using a micro-unit for membraneless gas diffusion. *Microchimica Acta* **2009,** *164* (1-2), 203-210.

33. Kunnecke, W.; Schmid, R. D., Development of a gas diffusion FIA system for on-line monitoring of ethanol. *J Biotechnol* **1990,** *14* (1), 127-40.

34. Mohns, J.; Kunnecke, W., Flow analysis with membrane separation and time based sampling for ethanol determination in beer and wine. *Analytica Chimica Acta* **1995,** *305* (1-3), 241-247.

35. Mattos, I.L.; Sartini, R. P.; Zagatto, E.A.G.; Reis, B. F.; Gin; Eacute; Fernanda, M., Spectrophotometric Flow Injection Determination of Ethanol in Distilled Spirits and Wines Involving Permeation through a Silicon Tubular Membrane. *Analytical Sciences* **1998,** *14* (5), 1005-1008.

36. Mattos,I. L.d.; Zagatto, E.A.G., Flow Systems Including Pervaporation for Spectrophotometric Monitoring of Ethanol in Industrial Fermentations. *Analytical Sciences* **1999,** *15* (1), 63-66.

37. Sereenonchai, K.; Saetear, P.; Amornthammarong, N.; Uraisin, K.; Wilairat, P.; Motomizu, S.; Nacapricha, D., Membraneless vaporization unit for direct analysis of solid sample. *Analytica Chimica Acta* **2007,** *597* (1), 157-162.

38. THITIMA BHUSRISOM, SELECTIVE AND HIGH THROUGHPUT QUANTITATION OF ETHANOL IN BEVERAGE USING SOME MEMBRANELESS VAPORIZATION APPARATUSES, Thesis, Mahidol university.

39. Skoog, Douglas A. Principles of instrumental analysis Philadelphia: Saunders College, c1998

40. Kompaney-Zareh M., Mansourian M., and Ravaee F. Simple method for colorimetric spot-test quantitative analysis of Fe (III) using a computer controlled hand-scanner. Analytica Chimica Acta 471 (2002) 97–104

41. L. Lahuerta Zamora, P. Aleman Lopez, G.M. Anton Fos, R. Martón Algarrac, A.M. Mellado Romero,and J. Martónez Calatayud. Quantitative colorimetric-imaging analysis of nickel in iron meteorites. Talanta 83 (2011) 1575–1579

42. Material Safety Data Sheet of Potassium dichromate, http://www.sciencelab.com/msds.php?msdsId=9927404.

APPENDIX A

Raw data from section 4.1

Reflectance was calculated by

$$R_x = -\log [I_x/I_{x,w}]$$

in which R_x= reflectance

x = color channel (red, greed, or blue)

w = white (blank)

Table A Raw data from each color channels

%EtOH	Red intensity	Red reflectance	Green intensity	Green reflectance	Blue intensity	Blue reflectance	Mean
0	203.73	0.00	77.77	0.00	1.37	0.00	0.00
5	168.49	0.08	44.29	0.24	1.36	0.00	0.11
10	127.77	0.20	23.87	0.51	3.28	-0.38	0.11
20	108.90	0.27	18.86	0.62	5.15	-0.58	0.10
30	62.27	0.51	10.68	0.86	6.83	-0.70	0.23
40	42.02	0.69	9.12	0.93	6.57	-0.68	0.31

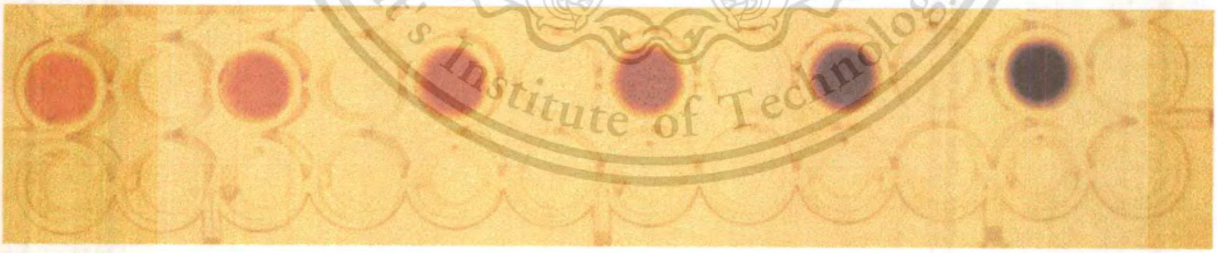

Figure A Standard ethanol and reagent

APPENDIX B

Optimization: Temperature (raw data from section 4.2.1)

Table B Results of study of optimization of temperature

Temperature (°C)	Linear relation	Linear correlation (R^2)
30	y = 0.0034x - 0.0177	0.9548
50	y = 0.0058x - 0.0486	0.8068
70	y = 0.017x - 0.0034	0.9839

Figure B1 standard ethanol and reagent at 30 °C

Figure B2 standard ethanol and reagent at 50 °C

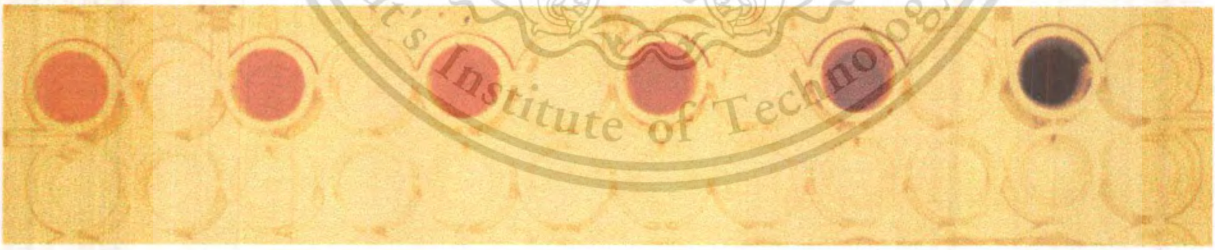

Figure B3 standard ethanol and reagent at 70 °C

APPENDIX C

Optimization: Diffusion time (raw data from section 4.2.2)

Table C Results of study of optimization of diffusion time

Time (minute)	Linear equation	Linear correlation (R^2)
3	$y = 0.0039x - 0.0286$	0.8334
5	$y = 0.0136x - 0.0785$	0.7299
7	$y = 0.017x - 0.0034$	0.9839
10	$y = 0.0263x + 0.0557$	0.9844

Figure C1 standard ethanol and reagent at diffusion time 3 min

Figure C2 standard ethanol and reagent at diffusion time 5 min

Figure C3 standard ethanol and reagent at diffusion time 7 min

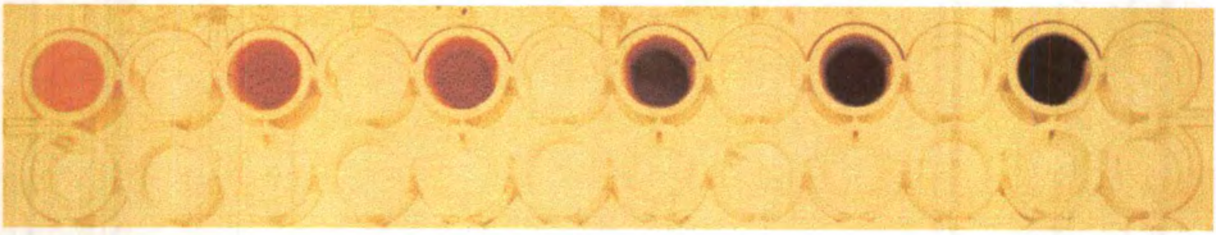

Figure C4 standard ethanol and reagent at diffusion time 10 min

APPENDIX D

Optimization: Concentration of reagents (raw data from section 4.2.3)

Table D1 Results of study of optimization of dichromate concentration

Dichromate's concentration (Mol/dm^3)	Linear equation	Linear correlation (R^2)
0.001M	y = 0.0016x - 0.0062	0.9541
0.005M	y = 0.0081x - 0.008	0.9798
0.01M	y = 0.017x - 0.0034	0.9839
0.05M	y = 0.0293x + 0.0178	0.9414

Figure D1 standard ethanol and reagent at concentration of dichromate 0.001 M

Figure D2 standard ethanol and reagent at concentration of dichromate 0.005 M

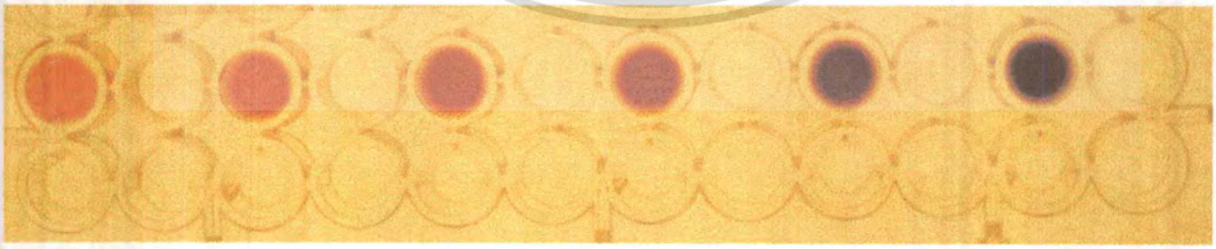

Figure D3 standard ethanol and reagent at concentration of dichromate 0.01 M

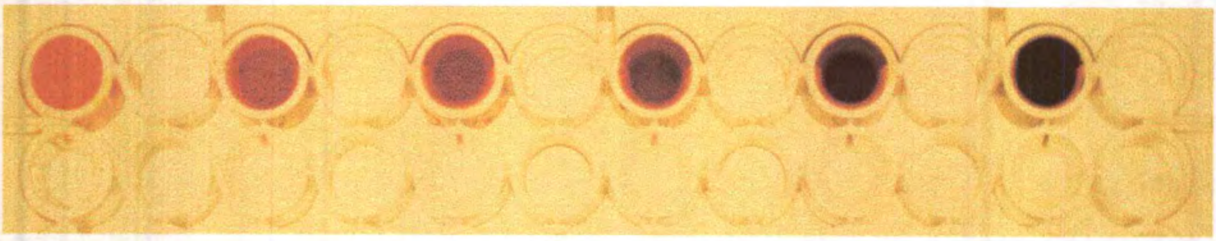

Figure D4 standard ethanol and reagent at concentration of dichromate 0.01 M

Table D2 Results of study of optimization of sulfuric acid concentration

Sulfuric acid's concentration	Linear equation	Linear correlation (R^2)
2.0M	y = 0.0095x - 0.0459	0.9313
2.5M	y = 0.0144x - 0.0576	0.9218
3.0M	y = 0.0198x - 0.0818	0.905

Figure D5 standard ethanol and reagent at concentration of sulfuric acid 2.0 M

Figure D6 standard ethanol and reagent at concentration of sulfuric acid 2.5 M

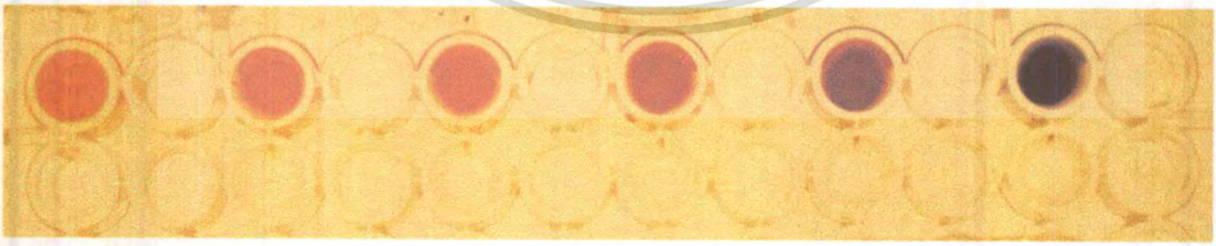

Figure D7 standard ethanol and reagent at concentration of sulfuric acid 3.0 M

APPENDIX E

Optimization: exposure value (raw data from section 4.2.4.1)

Table E Results of study of optimization of exposure value

Exposure	Linear equation	Linear correlation(R^2)
+2	y = 0.0122x - 0.0666	0.9028
+1	y = 0.0173x - 0.0804	0.9297
0	y = 0.0237x - 0.0937	0.9533
-1	y = 0.0283x - 0.0877	0.9779
-2	y = 0.0331x - 0.0857	0.9853

Figure E1 standard ethanol and reagent at exposure +2 eV

Figure E2 standard ethanol and reagent at exposure +1 eV

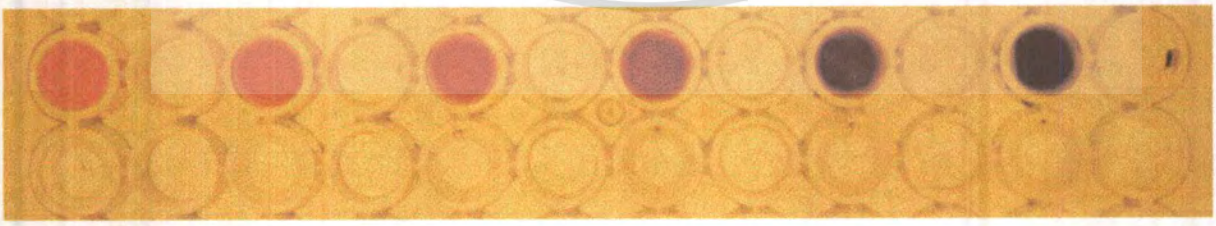

Figure E3 standard ethanol and reagent at exposure 0 eV

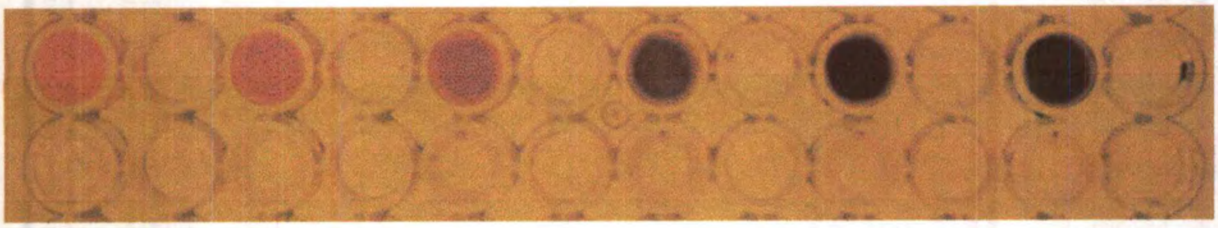

Figure E4 standard ethanol and reagent at exposure -1 eV

Figure E5 standard ethanol and reagent at exposure -2 eV

APPENDIX F

Optimization: ISO (raw data from section 4.2.4.2)

Table F Results of study of optimization of exposure value

ISO	Linear equation	Linear correlation(R^2)
100	y = 0.03x - 0.0883	0.958
200	y = 0.0315x - 0.0968	0.958
400	y = 0.0295x - 0.0838	0.9641

Figure F1 standard ethanol and reagent at ISO 100

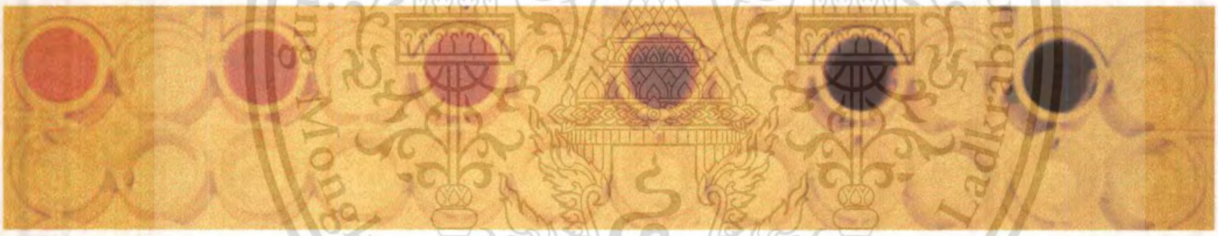

Figure F2 standard ethanol and reagent at ISO 200

Figure F3 standard ethanol and reagent at ISO 400

APPENDIX G

Precision (raw data from section 4.3.1.1 and 4.3.1.2)

$$RSD = \frac{SD}{\bar{x}} \times 100$$

Table G Results of precision study

Well No.	Intensity					Within well		
	1	2	3	4	5	Mean	SD	RSD
1	68.95	20.50	48.26	44.87	21.54	40.82	20.30	49.73
2	63.04	36.13	39.32	40.76	19.47	39.75	15.56	39.14
3	51.24	48.84	46.91	45.35	41.70	46.81	3.60	7.70
4	43.43	48.80	42.39	43.34	42.10	44.01	2.74	6.22
5	35.76	39.98	28.77	36.19	49.77	38.09	7.68	20.15
6	30.24	16.07	13.96	20.76	54.84	27.17	16.69	61.42
7	29.60	16.10	33.39	15.98	34.14	25.84	9.11	35.26
8	11.32	49.37	48.27	37.39	28.03	34.88	15.79	45.28
9	33.34	58.80	54.28	47.61	35.15	45.83	11.32	24.71
10	37.02	55.38	50.68	49.63	28.79	44.30	11.01	24.86
11	31.57	38.34	33.56	44.29	29.39	35.43	5.96	16.81
12	25.25	22.95	21.18	32.92	53.90	31.24	13.43	43.01
13	10.74	44.90	27.61	12.81	18.19	22.85	13.95	61.04
14	12.50	40.02	43.91	36.07	17.41	29.98	14.10	47.03
15	25.48	49.55	42.58	33.67	18.61	33.98	12.50	36.79
16	30.39	63.41	42.58	40.80	20.56	39.55	16.00	40.47
17	21.77	64.72	39.04	36.42	12.60	34.91	19.86	56.90
18	31.87	31.75	28.70	27.11	40.18	31.92	5.04	15.80
Mean	32.97	41.42	38.08	35.89	31.46			
SD	15.94	15.29	10.84	10.63	13.24			
RSD	48.34	36.90	28.46	29.63	42.07			
Between wells								

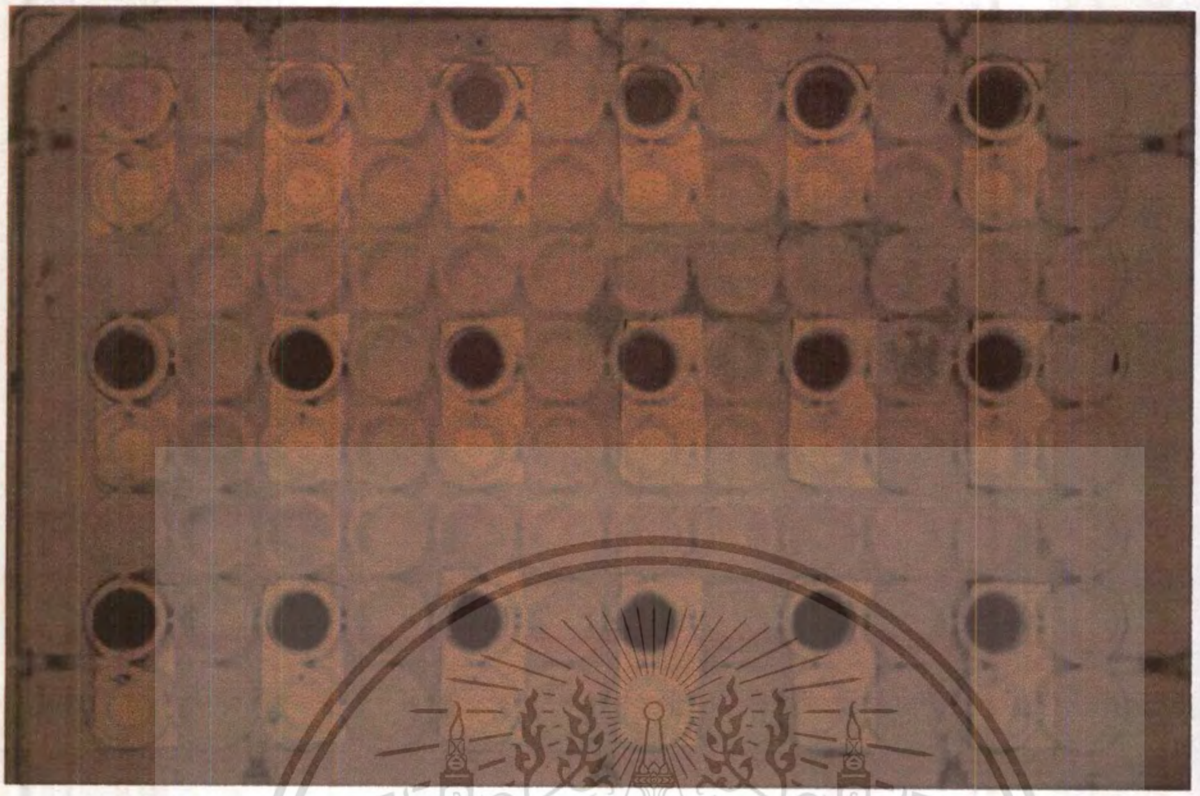

Figure G1 Precision study replicate 1

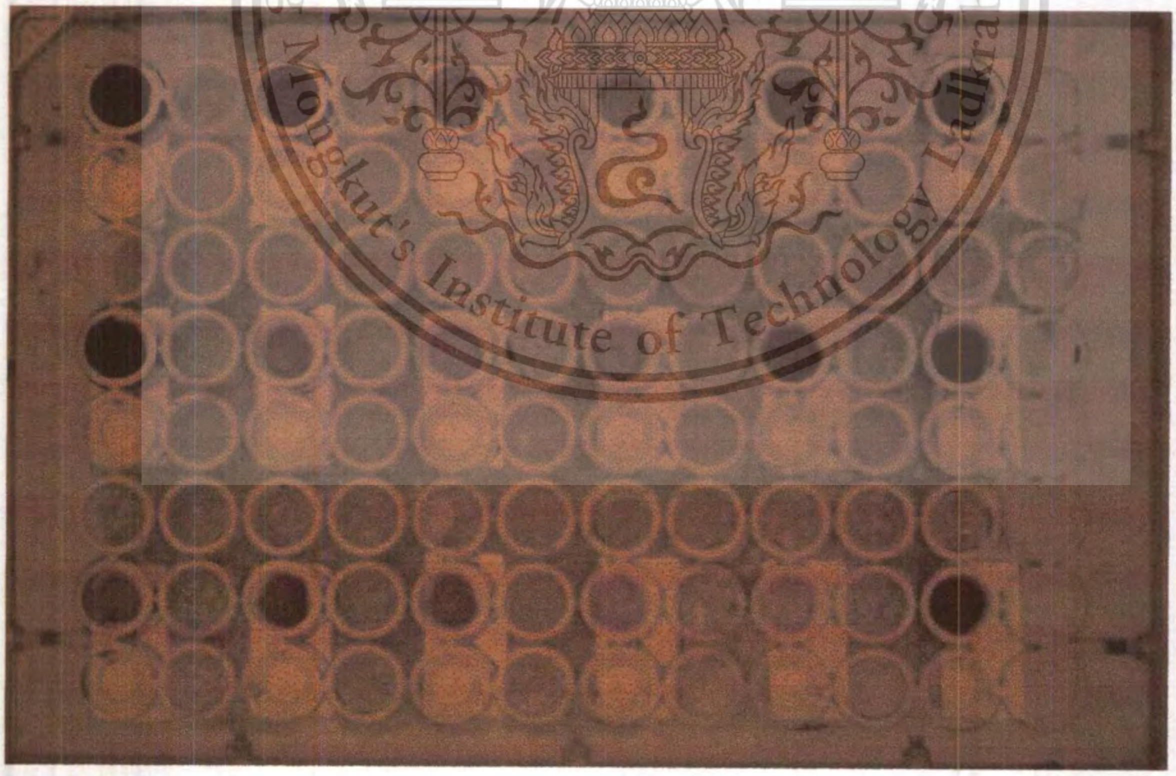

Figure G2 Precision study replicate 2

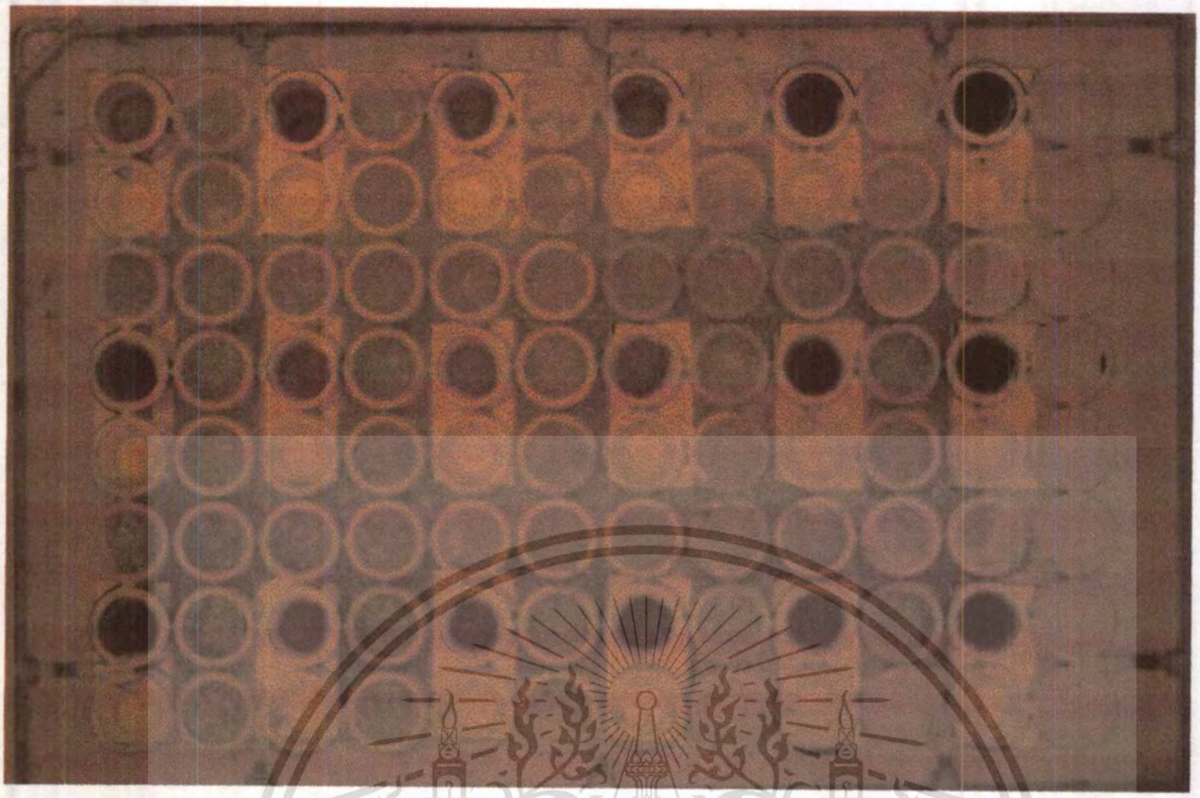

Figure G3 Precision study replicate 3

Figure G4 Precision study replicate 4

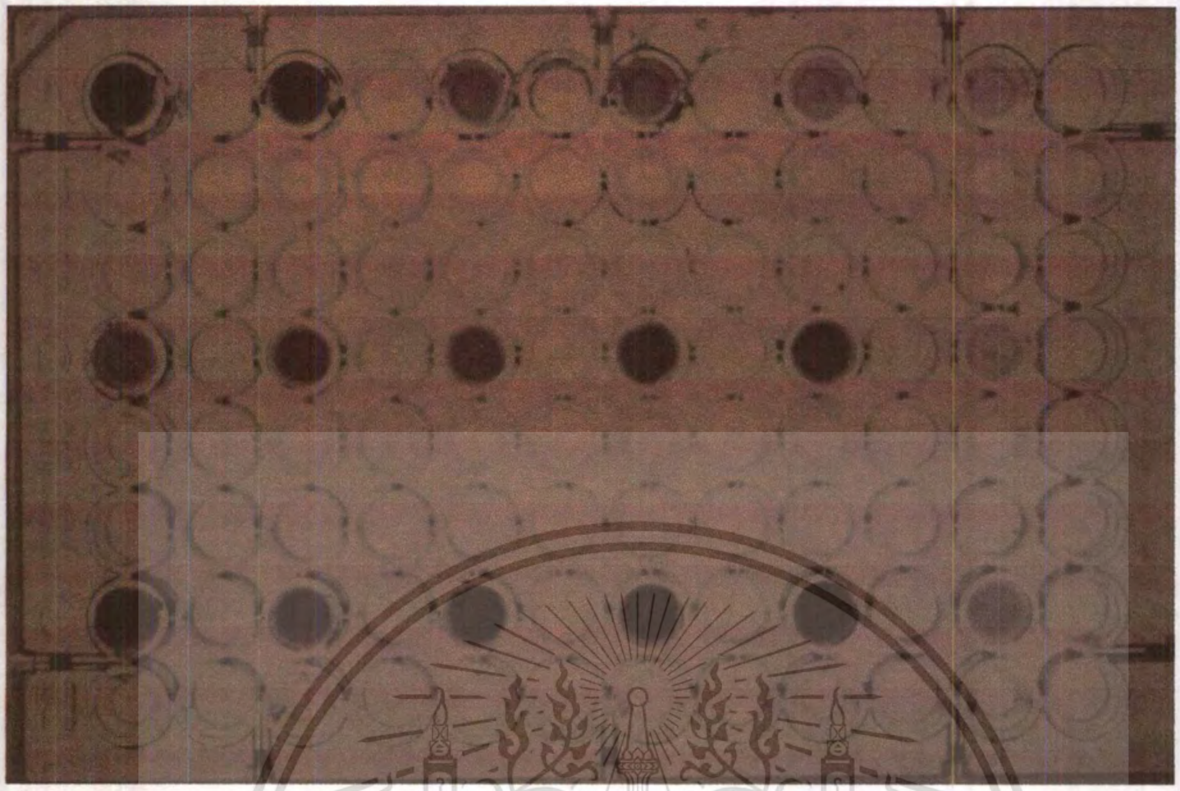

Figure G5 Precision study replicate 5

APPENDIX H

Limit of detection (raw data from section 4.3.2)

$$LOD = \frac{3SD_{Blank}}{Slope}$$

Table H Result from study on limit of detection

Intensity	Reflectance
86.379	0.040450555
91.849	0.013784295
87.543	0.034637302
84.047	0.052336511
78.075	0.084346734
76.707	0.092023729
80.983	0.068464866
84.88	0.048053356
90.743	0.019045594
90.012	0.022558316
87.728	0.033720499
83.231	0.056573615
SD	0.024968653
LOD	1.992179759

Calibration equation

y = 0.0376x - 0.1699

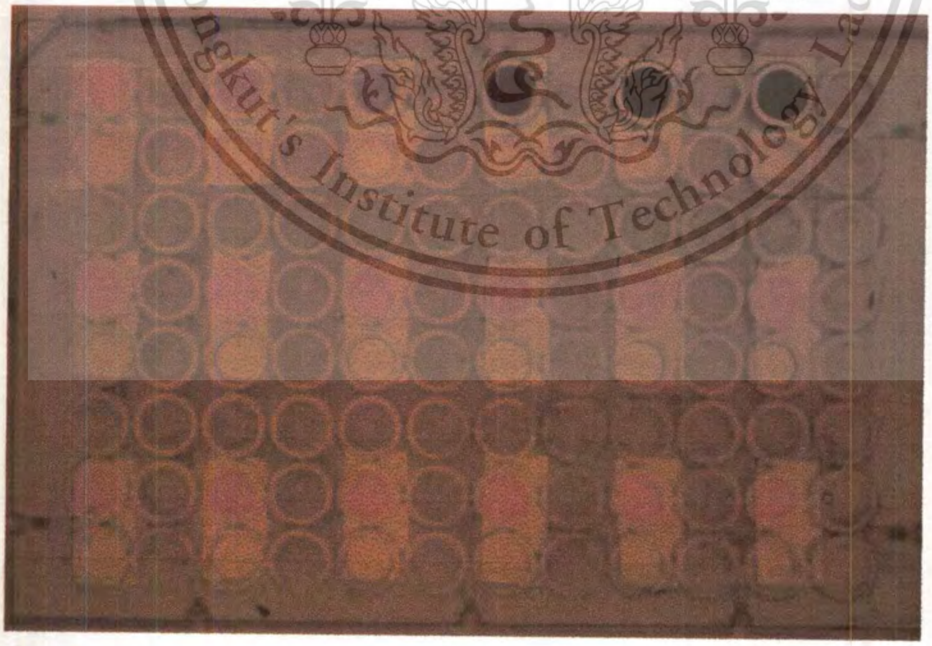

Figure H Top row is the standard ethanol and reagent used as a calibration curve.
Middle row and bottom rows are blank

APPENDIX I

Recovery data (raw data from section 4.3.3 and 4.3.4)

Raw data for sample No. 1-8

Table I1 Results of recovery study of sample 1

Sample	Intensity	Reflectance	%EtOH	Bottle
S1/1	56.84	0.18	8.32	10.40
	73.98	0.07	5.31	6.64
	74.82	0.06	5.18	6.47
S1/2	71.75	0.08	5.66	7.07
	62.09	0.15	7.31	9.14
	56.18	0.19	8.46	10.57
S1/3	61.54	0.15	7.41	9.27
	67.16	0.11	6.41	8.02
	72.85	0.08	5.48	6.86
		Mean	6.62	8.27
		SD	1.30	1.62

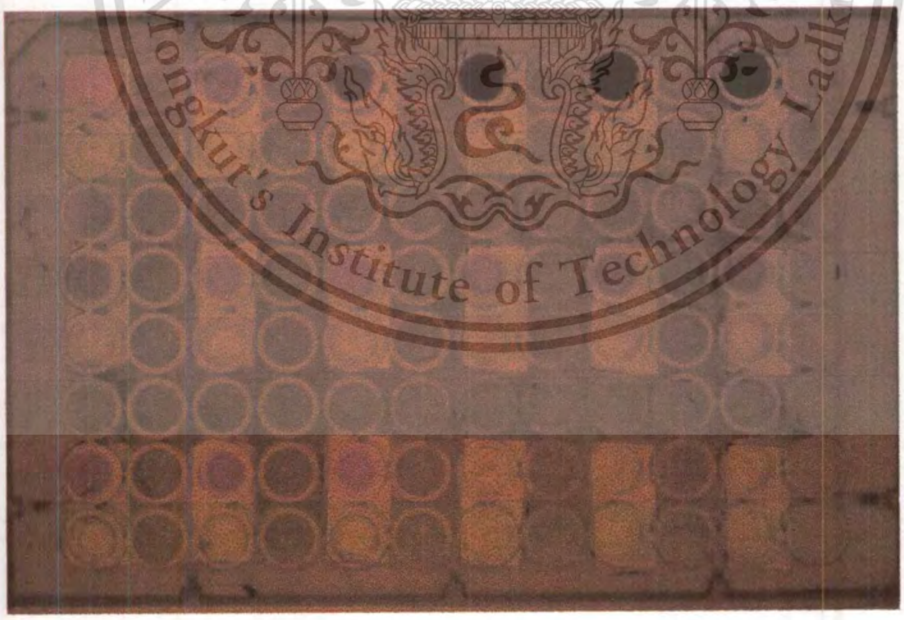

Figure I1 Top row is the standard ethanol and reagent used as a calibration curve.

Middle row is the standard ethanol with sample 1/1 and sample 1/2, respectively.
Bottom row is the standard ethanol and sample 1/3.

Table I2 Results of recovery study of sample 2

Sample	Intensity	Reflectance	%EtOH	Bottle
S2/1	58.56	0.21	6.53	8.17
	72.87	0.12	4.11	5.13
	77.28	0.09	3.45	4.32
S2/2	74.20	0.11	3.90	4.88
	64.85	0.17	5.40	6.75
	44.43	0.33	9.60	12.00
S2/3	74.00	0.11	3.93	4.92
	63.18	0.18	5.69	7.11
	63.33	0.18	5.66	7.08
		Mean	5.37	6.71
		SD	1.90	2.38

Figure I2 Top row is the standard ethanol and reagent used as a calibration curve.

Middle row is the standard ethanol with sample 2/1 and sample 2/2, respectively. Bottom row is the standard ethanol and sample 2/3.

Table I3 Results of recovery study of sample 3

Sample	Intensity	Reflectance	%EtOH	Bottle
S3/1	24.84	0.59	17.80	22.26
	38.45	0.40	13.18	16.47
	40.93	0.37	12.52	15.65
S3/2	36.90	0.41	13.61	17.02
	23.61	0.61	18.34	22.93
	14.27	0.83	23.68	29.60
S3/3	12.93	0.87	24.72	30.90
	23.51	0.61	18.39	22.98
	27.92	0.54	16.57	20.71
		Mean	17.65	22.06
		SD	4.35	5.43

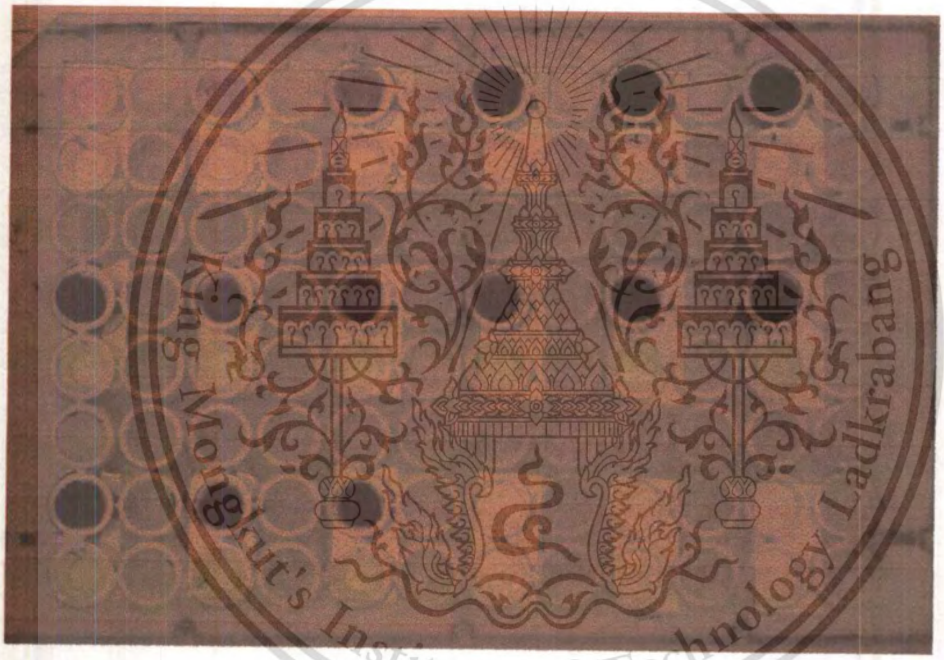

Figure I3 Top row is the standard ethanol and reagent used as a calibration curve.

Middle row is the standard ethanol with sample 3/1 and sample 3/2, respectively.
Bottom row is the standard ethanol and sample 3/3.

Table I4 Results of recovery study of sample 5

Sample	Intensity	Reflectance	%EtOH	Bottle
S5/1	23.76	0.61	26.06	32.57
	33.92	0.45	20.72	25.90
	38.54	0.40	18.81	23.51
S5/2	33.52	0.46	20.90	26.12
	18.51	0.72	29.80	37.25
	6.74	1.15	44.92	56.15
S5/3	25.88	0.57	24.78	30.97
	13.87	0.84	34.12	42.65
	16.35	0.77	31.66	39.57
		Mean	27.97	34.97
		SD	8.23	10.29

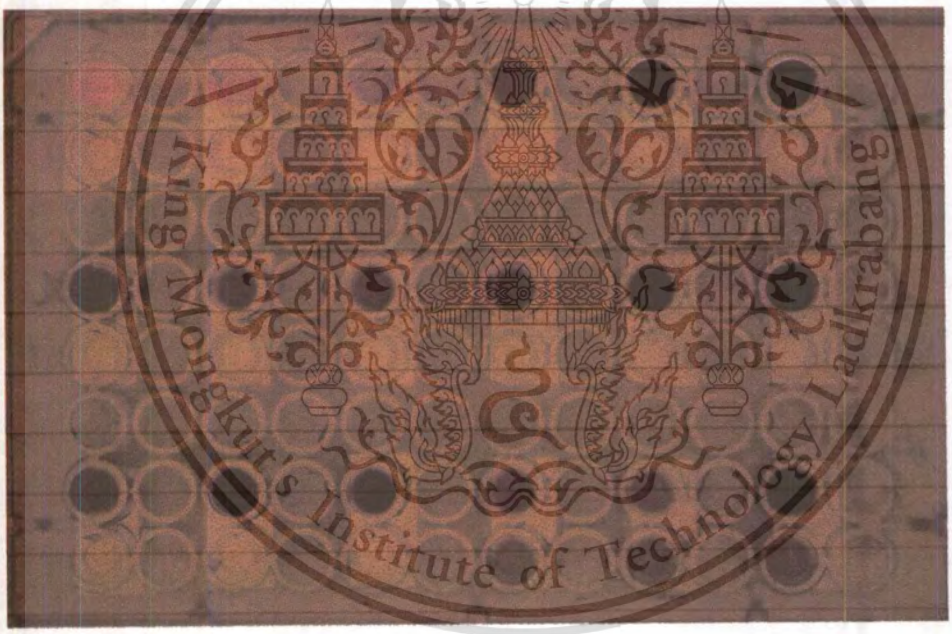

Figure I4 Top row is the standard ethanol and reagent used as a calibration curve.

Middle row is the standard ethanol with sample 5/1 and sample 5/2, respectively.
Bottom row is the standard ethanol and sample 5/3.

Table I5 Results of recovery study of sample 6

Sample	Intensity	Reflectance	%EtOH	Bottle
S6/1	85.49	0.04	3.48	4.34
	92.62	0.00	2.53	3.17
	90.99	0.01	2.74	3.43
S6/2	88.60	0.02	3.06	3.82
	81.84	0.05	3.99	4.99
	75.68	0.09	4.91	6.14
S6/3	85.16	0.04	3.52	4.40
	71.91	0.11	5.51	6.89
	85.65	0.03	3.45	4.32
		Mean	3.69	4.61
		SD	0.98	1.22

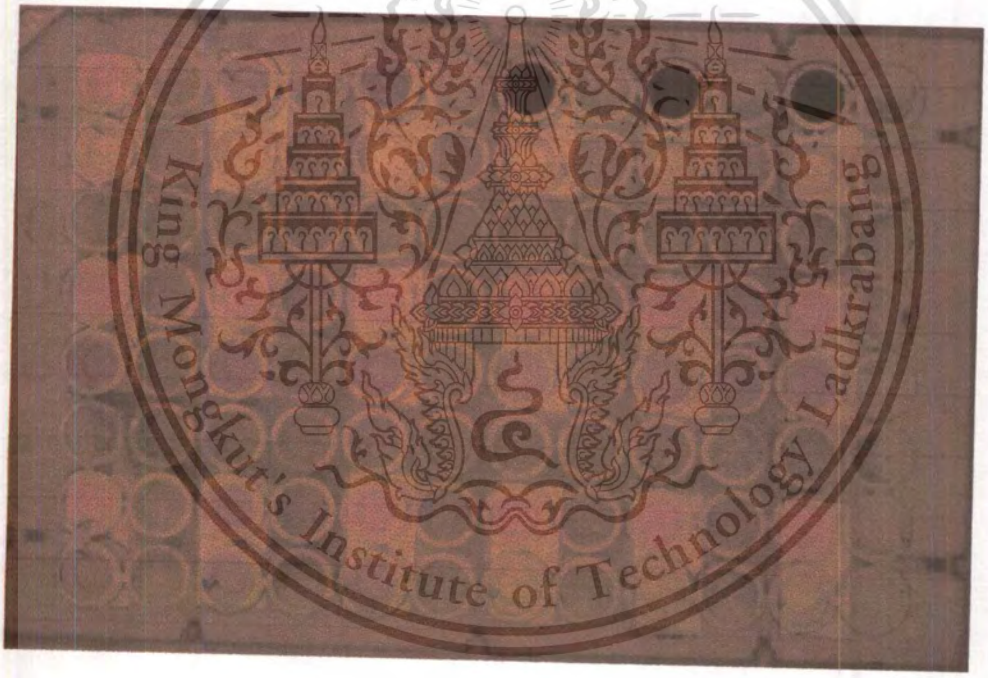

Figure I5 Top row is the standard ethanol and reagent used as a calibration curve.

Middle row is the standard ethanol with sample 6/1 and sample 6/2, respectively. Bottom row is the standard ethanol and sample 6/3.

Table I6 Results of recovery study of sample 4, 7 and 8

Sample	Intensity	Reflectance	%EtOH	Bottle
S4	14.84	0.74	25.24	31.54
	23.06	0.55	20.07	25.08
	34.85	0.37	15.22	19.02
		Mean	20.17	25.21
		SD	5.01	6.26
S7	74.21	0.05	6.35	7.93
	79.92	0.01	5.48	6.84
	74.50	0.04	6.30	7.88
		Mean	6.04	7.55
		SD	0.49	0.62
S8	75.36	0.04	6.16	7.71
	79.24	0.02	5.58	6.97
	83.83	-0.01	4.92	6.14
		Mean	5.55	6.94
		SD	0.63	0.79

Figure I6 Top row is the standard ethanol and reagent used as a calibration curve.

Middle row is the standard ethanol with sample 4 and sample 7, respectively. Bottom row is the standard ethanol and sample 8.

Table I7 Results of recovery study of spiked sample 1

Sample	Intensity	Reflectance	%EtOH
S 1/1	46.55	0.26	11.42
	41.01	0.32	12.81
	34.77	0.39	14.62
S1/2	23.34	0.56	19.00
	15.06	0.75	23.80
	17.34	0.69	22.25
S1/3	11.19	0.88	27.05
	23.03	0.57	19.14
	21.41	0.60	19.94
		Mean	18.89
		SD	5.17

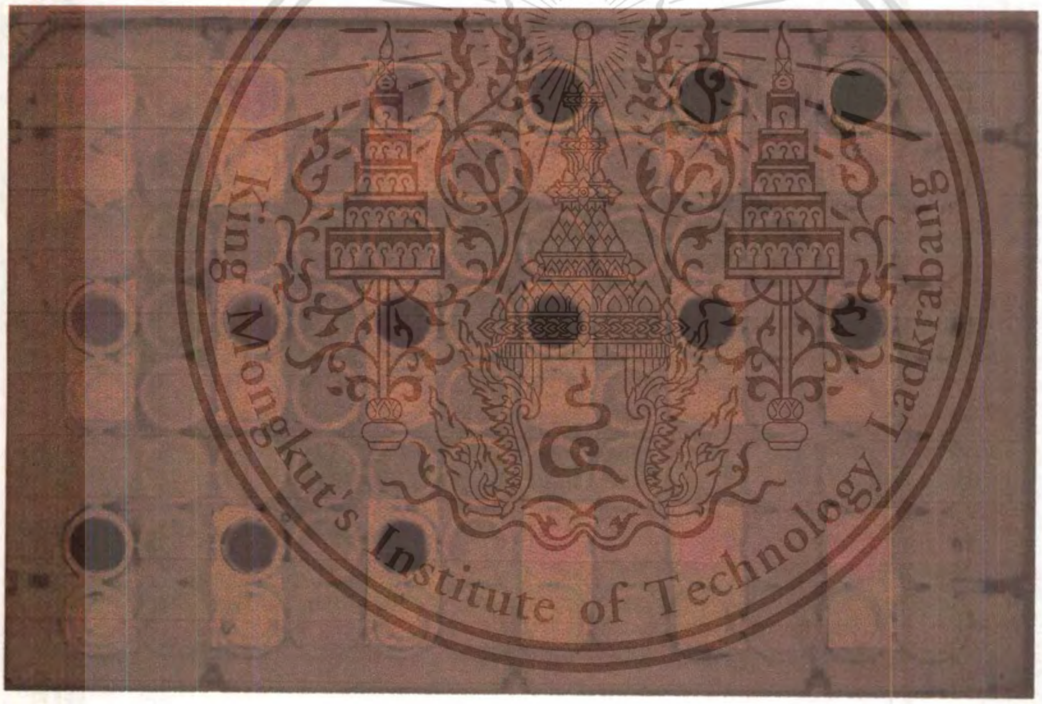

Figure I7 Top row is the standard ethanol and reagent used as a calibration curve.

Middle row is the standard ethanol with spiked sample 1/1 and 1/2, respectively. Bottom row is the standard ethanol and spiked sample 1/3.

Table I8 Results of recovery study of spiked sample 2

Sample	Intensity	Reflectance	%EtOH
S2/1	57.76	0.21	10.56
	56.65	0.22	10.86
	52.02	0.25	12.16
S2/2	45.59	0.31	14.17
	42.87	0.34	15.11
	32.20	0.46	19.47
S2/3	21.30	0.64	25.77
	15.44	0.78	30.67
	39.39	0.37	16.40
		Mean	17.24
		SD	6.93

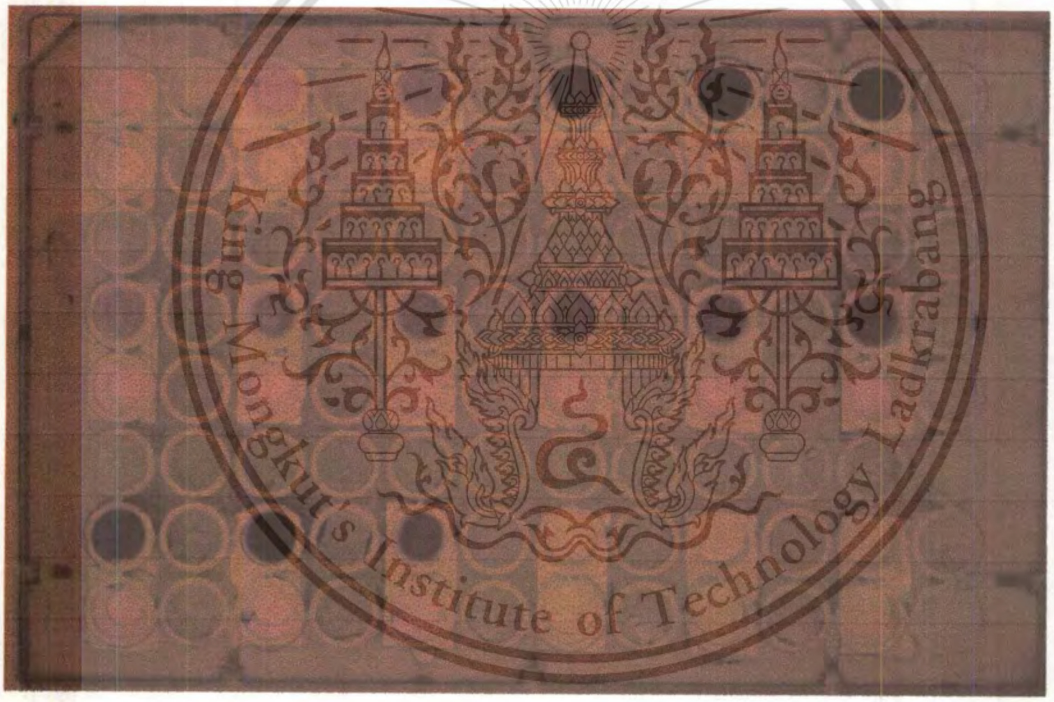

Figure I8 Top row is the standard ethanol and reagent used as a calibration curve.

Middle row is the standard ethanol with spiked sample 2/1 and 2/2, respectively. Bottom row is the standard ethanol and spiked sample 2/3.

Table I9 Results of recovery study of spiked sample 3

Sample	Intensity	Reflectance	%EtOH
S3/1	7.09	1.03	32.50
	9.75	0.89	28.10
	14.46	0.72	22.64
S3/2	15.10	0.70	22.04
	13.68	0.74	23.41
	10.63	0.85	26.90
S3/3	12.25	0.79	24.94
	7.47	1.00	31.77
	8.69	0.94	29.69
		Mean	26.89
		SD	0.12

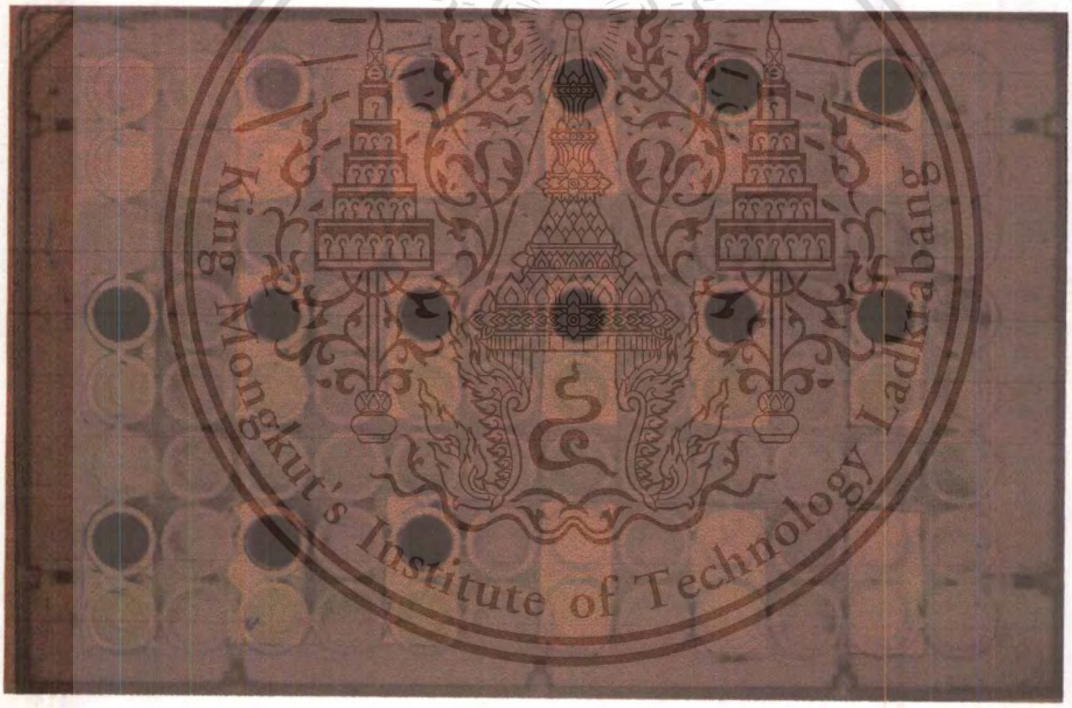

Figure I9 Top row is the standard ethanol and reagent used as a calibration curve.

Middle row is the standard ethanol with spiked sample 3/1 and 3/2, respectively. Bottom row is the standard ethanol and spiked sample 3/3.

Table I10 Results of recovery study of spiked sample 5

Sample	Intensity	Reflectance	%EtOH
S5/1	11.15	0.90	30.78
	14.45	0.79	27.07
	13.65	0.81	27.88
S5/2	14.38	0.79	27.15
	9.20	0.99	33.52
	15.32	0.76	26.24
S5/3	13.51	0.82	28.04
	14.29	0.79	27.23
	13.58	0.82	27.96
		Mean	28.43
		SD	2.29

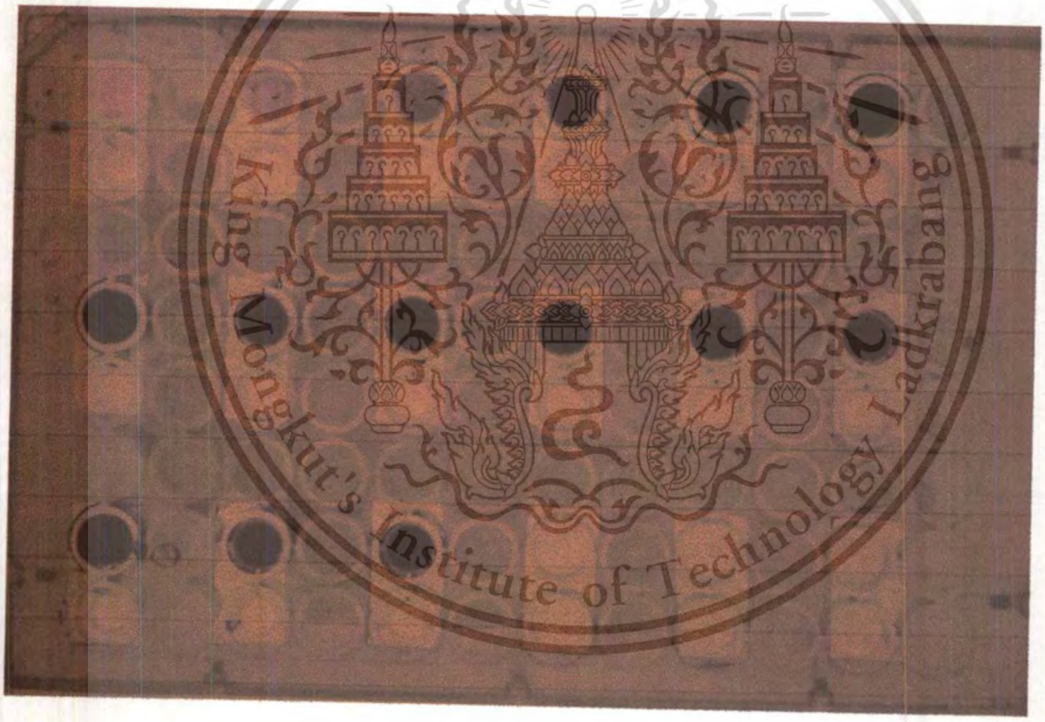

Figure I10 Top row is the standard ethanol and reagent used as a calibration curve.

Middle row is the standard ethanol with spiked sample 5/1 and 5/2, respectively.
Bottom row is the standard ethanol and spiked sample 5/3.

Table I11 Results of recovery study of spiked sample 6

Sample	Intensity	Reflectance	%EtOH
S6/1	51.85	0.23	8.49
	54.45	0.21	7.60
	44.38	0.30	11.30
S6/2	41.23	0.33	12.64
	36.23	0.39	14.97
	28.25	0.50	19.47
S6/3	18.13	0.69	27.50
	25.70	0.54	21.19
	37.99	0.37	14.11
		Mean	15.25
		SD	6.43

Figure I11 Top row is the standard ethanol and reagent used as a calibration curve.

Middle row is the standard ethanol with spiked sample 6/1 and 6/2, respectively. Bottom row is the standard ethanol and spiked sample 6/3.

Table I12 Results of recovery study of spiked sample 4, 7 and 8

Sample	Intensity	Reflectance	%EtOH
S4	28.29	0.51	19.93
	18.02	0.70	25.15
	28.72	0.50	19.76
S7	30.05	0.48	19.23
	13.30	0.84	28.67
	26.71	0.53	20.60
S8	38.95	0.37	16.23
	11.73	0.89	30.13
	13.69	0.82	28.34
		Mean	23.11
		SD	5.02

Figure I12 Top row is the standard ethanol and reagent used as a calibration curve.

Middle row is the standard ethanol with spiked sample 4 and 7, respectively.
Bottom row is the standard ethanol and spiked sample 8.